UNITED NATIONS UNIVERSITY
GEOTHERMAL TRAINING PROGRAMME
Orkustofnun, Grensásvegur 9,
IS-108 Reykjavík, Iceland

Reports 2009
Number 20

THE POTENTIAL RELATIONSHIP OF SOME GEOTHERMAL FIELDS IN UGANDA

Deus Katomi Muhwezi
Department of Geological Survey and Mines
Ministry of Energy and Mineral Development
P.O. Box 9, Entebbe
UGANDA
deuskatomi@yahoo.com

ABSTRACT

Detailed geological work has concentrated on three main geothermal areas of southwest Uganda: Katwe-Kikorongo, Buranga and Kibiro hot springs. This has included geochemical exploration, isotope hydrology, geological mapping and geophysics. Using resistivity measurements, anomalies were located in Katwe and Kibiro, thought to delineate a geothermal reservoir. However, drilling of geothermal gradient wells gave no sign of geothermal activity. Hence, there is a need to expand the previously targeted areas for drilling and to probe deeper. In this project, a study was carried out to correlate different geothermal hot springs with the aim of grouping them into geothermal fields. The characteristics of the geothermal fluids were studied using Cl-SO_4-HCO_3, Na-K-Mg, Cl-Li-B ternary diagrams, speciation using the WATCH program, isotopes, and ratios between conservative elements and mixing models. The Cl-SO_4-HCO_3 ternary diagram was employed to classify Amoropii, Okumu, and Kibiro as chloride waters, Kitagata and Kanangorok as steam heated waters, Kibenge, Kabuga and Rwagimba as volcanic waters, but Amuru, Amuru (Pakele) and Avuka as peripheral bicarbonate waters. The source of geothermal fluids is old base rock rather than underlying sediments and the fluids are partially or fully equilibrated. . The δ^2H versus $\delta^{18}O$ plots and the Cl/B, Cl/Li, Na/K, Na/Cl ratios show that Kibenge, Rwagimba and Kabuga are correlated to Buranga with fluids of similar origin while Kibiro and Panyamur appear to be linked, with Avuka at the periphery of the Kibiro-Panyamur geothermal area. SiO_2-CO_2 mixing models show that there was no boiling in the hot springs studied but there was some evidence of mixing. The log Q temperature plots for minerals show that Kanangorok, Kabuga, Kibenge, Rwagimba, and Okumu are saturated with calcite and could be prone to scaling if utilised.

1. INTRODUCTION

Uganda is one of the east African counties crosscut by the East African Rift System. Several geological surveys, including shallow drilling, have been carried out in three geothermal areas of Uganda, Katwe-Kikorongo, Buranga and Kibiro. Preliminary work has also been carried out in other geothermal areas of Uganda, aimed at using the geothermal energy for rural development. Biomass represents 93% of the energy used in the country, installed capacity of thermal power is 100 MWe and

installed hydroelectric power is 380 MWe but has decreased to150 MWe in the past few years due to climatic changes. This has made electricity expensive and unaffordable besides being scarce. Since all oil products are imported, the government is considering the development of renewable energy; geothermal energy with an estimated capacity of 450 MW_e (McNitt, 1982) is one of the key players.

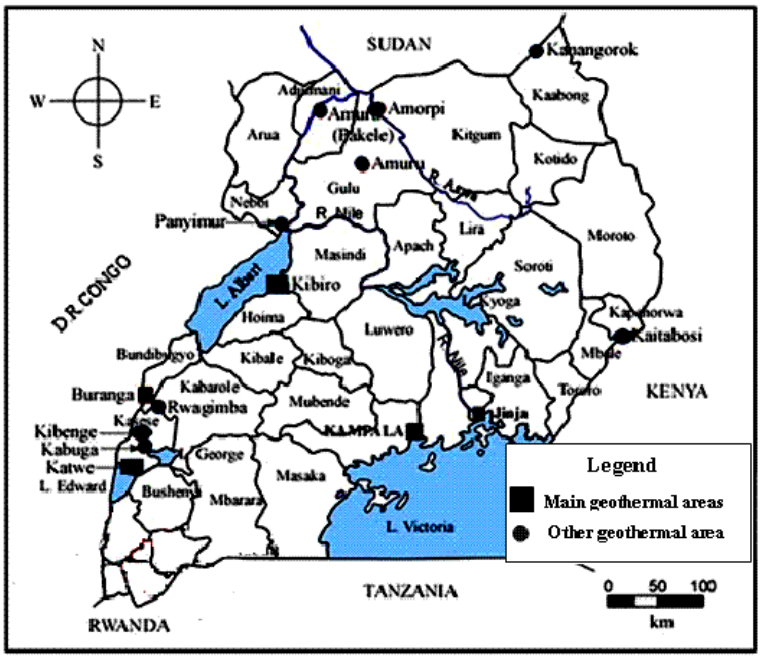

FIGURE 1: Map of Uganda showing the location of hot springs studied (Bahati and Natukunda, 2008)

This study covers the three main geothermal areas: Katwe-Kikorongo (Katwe), Buranga and Kibiro, but also Kibenge, Kabuga, Rwagimba and the northern Uganda hot springs i.e. Amuru, Avuka Amuru (Pakele), Amoropii, and Kanangorok. These are all located in the Western Rift Valley in the Albertine graben that runs along the border of Uganda and the Democratic Republic of Congo (Figure 1).

During geological, geophysical, and geochemical exploration, anomalies for drilling were located in the Katwe-Kikorongo, Buranga and Kibiro geothermal fields. However, drilling to the depth indicated by geophysical methods to give a relatively high temperature in Katwe-Kikorongo and Kibiro gave much lower geothermal gradients than expected and there was no sign of geothermal activity to be inferred from the drill cores. It was, however, thought that the low resistivity could be due to an ore mineral body in the case of Kibiro and salt deposits in the case of Katwe-Kikorongo. It was concluded that the source of heat was likely to be deeper or outside the areas previously interpreted as drilling targets. The future plan is to use geophysical methods that probe deeper to expand the study area and compare geothermal hot springs to find if there could be a link between the main geothermal hot springs and other neighbouring hot springs.

The objective of the present project is to analyse and correlate the geochemical data for different hot springs, to find possible potential with reference to geological location and structural controls. These were considered in two groups: firstly Buranga, Katwe-Kikorongo, Kibenge, Kabuga and Rwagimba, and secondly Kibiro (Figure 2) and the northern Uganda hot springs (Amuru, Amuru (Pakele), Amoropii, Avuka and Kanangorok). To find out whether there was a relationship between fluids of different hot springs, their chemical compositions were studied by looking at the conservative constituents that can be regarded as tracers. These included Li, Rb, which are highly mobile, and Cl, B, and Br which form soluble minerals and whose supply sources to geothermal fluids are too limited for saturation with regard to any mineral (Arnórsson, 2000a).

Deuterium was also used as a conservative isotope in the geothermal fluids due to its mobility. The formation of secondary minerals containing water can cause deuterium to fractionate between mineral and water. However, the amount of water held in secondary minerals is insignificant compared to the amount flowing through a given rock, hence fractionation between the phases will have negligible effect on the deuterium content of water flowing through it. Also water with temperature below 100°C generally shows no oxygen isotope shift and hence the ^{18}O isotope can be used as a tracer. Sulphate can also be reactive in some geothermal systems as it can react and be precipitated as anhydrite but is conservative in others (Arnórsson, 2000a).

2. GELOGICAL BACKGROUND AND LITERATURE REVIEW

2.1 The geology of the three main geothermal fields

Kibiro geothermal field

The Kibiro geothermal field is divided into two geological environments by an escarpment of the western branch of the east African Rift Valley that runs northeast to southwest. The eastern side is mainly a crystalline basement with granites and granitic gneisses while the western part is characterised by rift sediments. The hot springs are found in the rift sediments (Figure 2). Kachuru fault trending NNE-SSE is oblique to the main rift fault and intersects it at Kachuru and Kibiro villages. Several surface manifestations are found at the intersection of the two faults (Figure 3). The surface manifestations entail hot and warm springs which include Mukabiga and Mwibanda; there are also salt gardens such as the Muntere salt

FIGURE 2: Kibiro hot springs in rift sediments

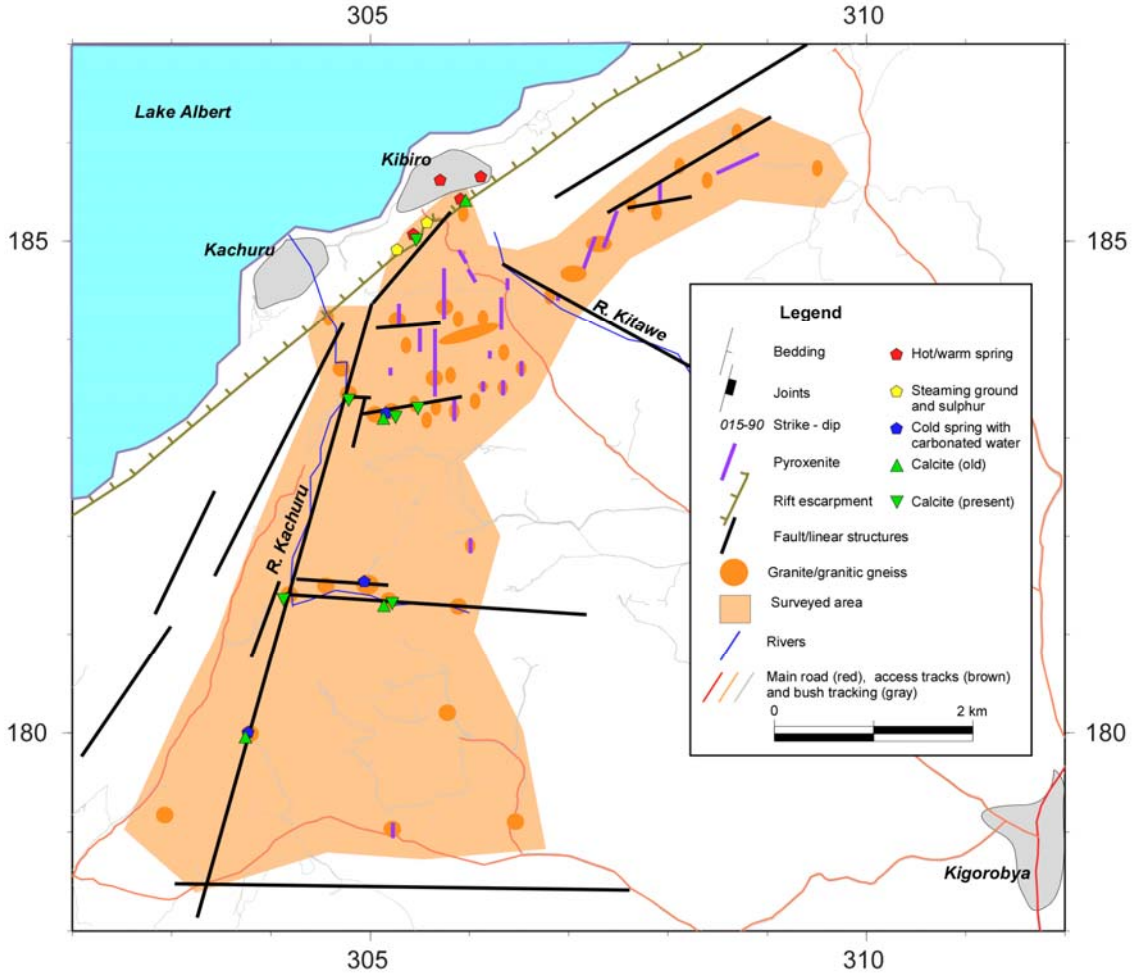

FIGURE 3: Geology of the Kibiro area (Gíslason et al., 2004)

garden. Other manifestations include hydrogen sulphide emissions, steaming grounds, calcite and sulphur deposits (Gíslason et al., 2004; Gíslason, 1994)

Katwe-Kikorongo geothermal field

The Katwe-Kikorongo volcanic field is located on the escarpment of the western branch of the East African Rift Valley south of Rwenzori massif. The field has a number of craters that lie on the NE-SW striking main fault. It is characterised by basement granite and granite gneisses (Figure 4), explosion craters, ejected pyroclasts and tuffs (Figure 5). The craters are believed to have been formed by phreatic eruptions and in some of them, like Lake Katwe, Kikorongo and Nyamunuka, there are crater lakes with high salinity due to evaporation (Figure 5). There are also minor occurrences of lava near Lake Kitagata and Kyemengo crater areas. Geothermal surface manifestations are scarce and only found in the Katwe and Kitagata craters.

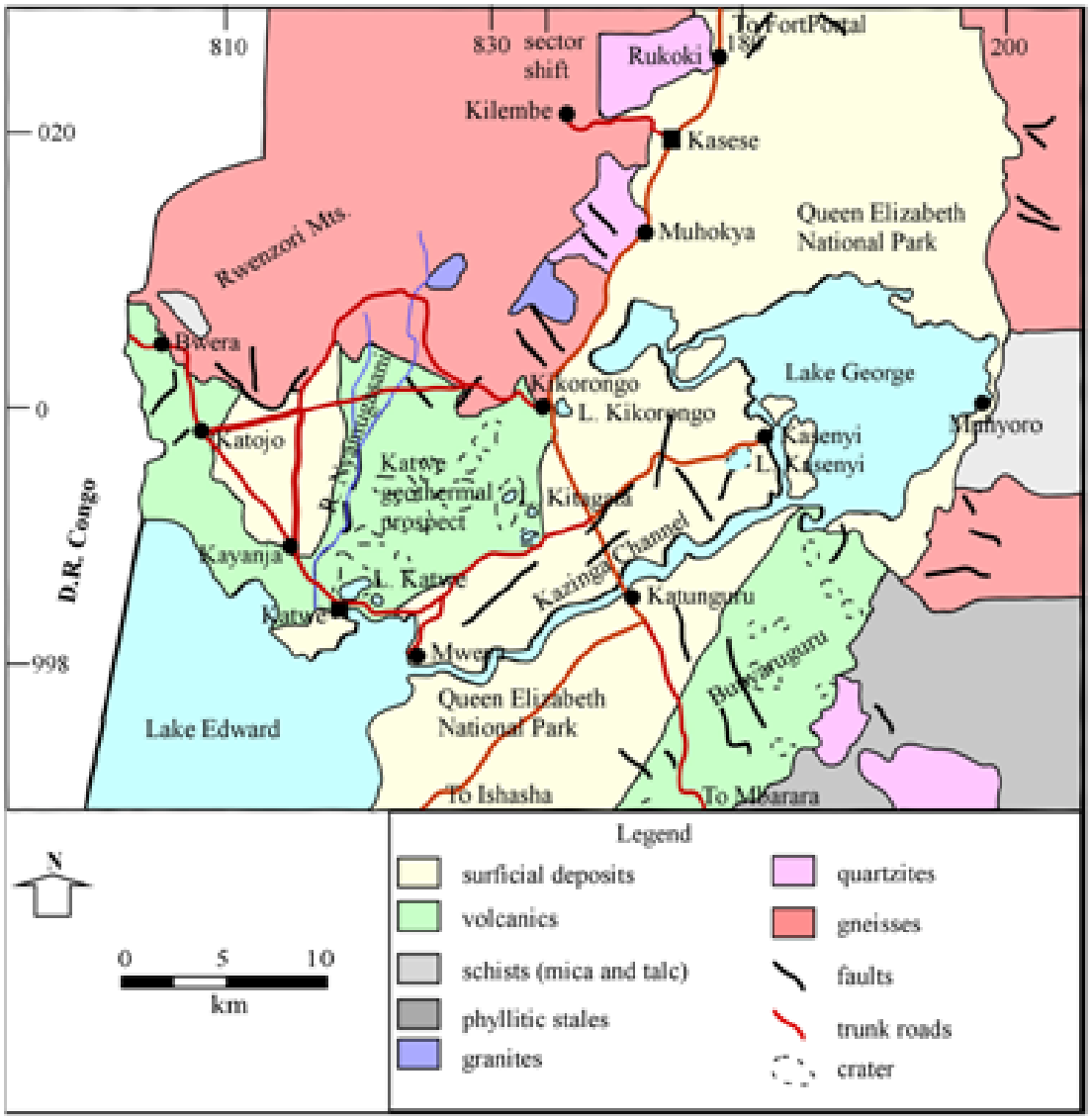

FIGURE 4: Map of the geology of Katwe-Kikorongo area
(Bahati and Natukunda, 2008)

Buranga geothermal field

This field is also in the western branch of the East African Rift Valley. It is situated in a sedimentary environment (Figure 6) and, despite high tectonic activity, Buranga has no evidence of volcanism. It is a geothermal field with spouting hot springs, high gas flow and travertine deposits.

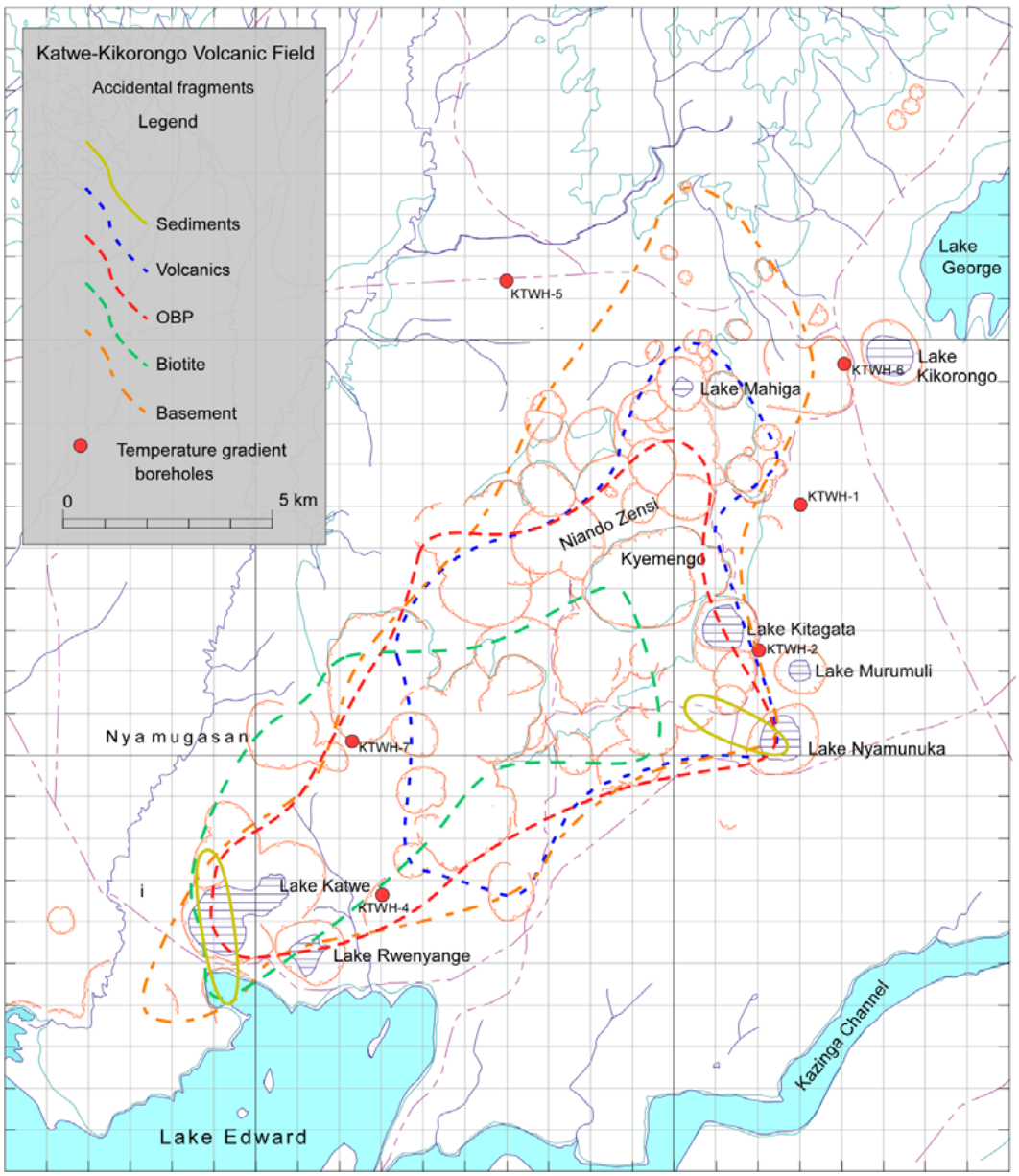

FIGURE 5: Katwe-Kikorongo geothermal field showing springs and craters (Bahati and Natukunda, 2008)

2.2 Geology of other hot spring areas

Kabuga hot spring (also called Muhokya warm springs) has a temperature of about 40°C and a flow rate of 1 l/s. It has no rock exposure but the surface geology indicates that the springs issue from alluvial and pediment gravel material at the base of the Rwenzori mountains. Kabuga is also thought to be controlled by the major Rwenzori fault that extends from Lake Kitagata in the Katwe geothermal field (Bahati et al., 2005).

Panyamur hot springs are located on the escarpment near the shores of Lake Albert. They are divided into three hot springs which include Amoropii, Okumu and Avuka. All three lie on the Rift Valley escarpment. They extend in a northwesterly direction and are likely to be controlled by a major boundary fault.

The manifestations include hot springs, travertine deposits, sulphurous algae and hydrogen sulphide emissions. From the hot spring there lies a gorge that dips into the escarpment in which fractured

crystalline basement rocks like coarse hornblende gneiss, coarse hornblende garnet rock, and talcose rock have been reported. There are two directions of foliation, NNE-SSW and NE-SW, in the direction of the local major fault. Okumu is characterised by basement rocks of granitic gneiss and Pleistocene sediments to the east of the rift fault boundary. Amuru is underlain by fractured basement rocks with foliation trending NNE-SSW and joints trending NE-SW in quartzite.

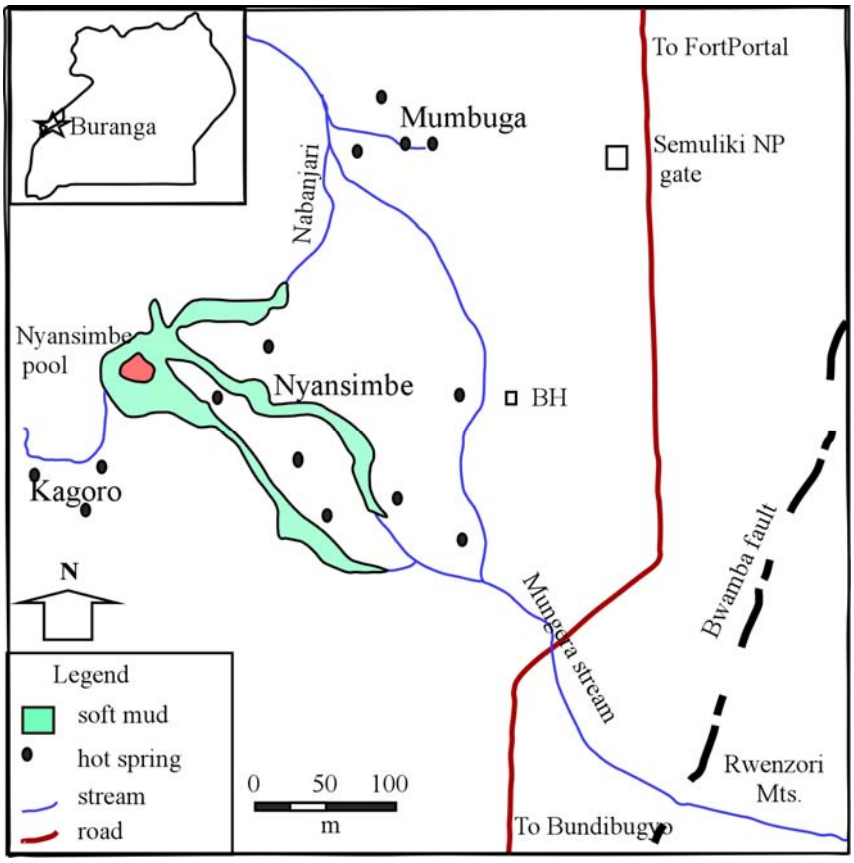

FIGURE 6: Map of the Buranga geothermal field (Gíslason, 1994)

2.3 Literature review

Geothermal exploration started in Uganda way back in 1921 but serious work started in 1993 -1994 with the UGA/92/002 project funded by UNDP (Gíslason, 1994). From this project I will only concentrate on the geochemistry (Ármannsson, 1994). The exploration work was confined to three main geothermal areas: Katwe-Kikorongo, Buranga and Kibiro. In Buranga there is chloride-sulphate-carbonate water, in Kibiro alkali chloride water while in Katwe there are volcanic sulphate waters. On the Cl-Li-B diagram, all plotted near the chloride corner showing low boron. Hence, the fluids are likely to have resided in rock rather than sediments. The hydrogen sulphide from the hot springs is apparently geothermal. Katwe-Kikorongo geothermal fluids are saline with a subsurface temperature of 100-150°C inferred by geothermometers. However, there are some indicators of temperature in excess of 200°C. Buranga has an estimated subsurface temperature of 120-150°C while in Kibiro the geochemistry suggested that the surface fluids are a mixture of 70% geothermal component and 30% groundwater. The geothermal fluid end-member is probably saline with a temperature of about 200°C. Geophysical exploration to determine the size of the Kibiro field was recommended (Ármannsson, 1994). More work was carried out under the IAEA TC-PROJECT UGA/8/OO3 on hydrology and reservoir characteristics of Katwe, Kibiro and Buranga. Under the project hot water, cold water and rock samples were analysed for chemical constituents and isotopes of hydrogen (δ^2H_{H2O}, $^3H_{H2O}$), oxygen ($\delta\ ^{18}O_{H2O}\ ^{18}O_{SO4}$), carbon ($\delta^{13}C_{DIC}$, $^{14}C_{DIC,}$ where DIC represents dissolved inorganic carbon), sulphur ($\delta^{34}S_{SO4}$), and strontium ($^{87/86}Sr_{H2O}$, $^{87/86}\ Sr_{Rock}$). The results showed that the circulating water in the geothermal system was of meteoric origin. Katwe-Kikorongo, Buranga and Kibenge geothermal areas are most likely charged from Rwenzori Mountains with Katwe water likely to be a mixture of local groundwater, water from the Rwenzori Mountains and lake water. Kibiro is recharged by water either from east of Kibiro or the Mukihani-Waisembe ridge located southeast of Kibiro. Isotope geothermometers predicted 200°C for Buranga, 130-140°C for Katwe-Kikorongo and 110-135°C for Kibiro. Kibiro temperature was low and most probably due to mixing with relatively sulphate rich groundwater. The reservoir rock types were found most likely to be basalt (leucite and melilites) with ultramafic xenoliths in Katwe-Kikorongo, and granitic gneiss in Buranga and Kibiro. The results also showed no sign of oxygen isotope shift for the hot spring

waters, suggesting high permeability. There is a slight oxygen isotope shift in Katwe Kikorongo which could be due to mixing with lake water, while in Kibiro there is an insignificant oxygen isotope shift (Bahati et al., 2005; Bahati, 2007).

Under the GEOTHERM programme funded by the Government of Germany, samples from the Rwenzori hot springs that included Lake Kitagata, Muhokya, Kibenge, Bugoye, Rwimi, Rwagimba, Nyansimbe, Kagoro, Mbuga, and Kibuku were analysed. It was found that Buranga has no detectable tritium, and that the Rwenzori springs had a predicted subsurface temperature of 150°C. Most of the Rwenzori hot springs deposited travertine with the exception of Kibenge and Muhokya. Isotope results for Buranga, Katwe and Muhokya travertine were plotted on a $^{13}C/^{12}C$ versus $^{18}O/^{16}O$ plot, which plotted in the carbonatite region, showing that the carbon in the carbon dioxide which reacted with fluids to precipitate travertine derived from magma. The strontium values also indicated an interaction of fluid with granite gneiss. From the study it was concluded that the fluids in Buranga, Rwimi, Kibuku, and the foot craters with high bicarbonate and low silica could constitute an out-flow of a geothermal system in the Rwenzori Mountains. It was recommended that a study of stable isotopes should be carried out on the Rwenzori hot springs to find the relationship (Kato and Kraml, 2005).

Kato and Kraml (2005) carried out a trace element analysis on Buranga travertine deposits and found that they contained an unusually large amount of Ba (1200, 884, 772.9ppm) compared to the Muhokya limestone deposit (34.2 ppm)which is sedimentary in origin. Travertine deposits from juvenile source are rich in Ba and this origin was supported by isotope values ($^{18}O/^{16}O$ = -18.6, $^{13}C/^{12}C$ = -7.8). The travertine also had no detectable Sr concentrations, unlike the sedimentary equivalents.

Exploration of other geothermal hot springs in southwest Uganda began by visiting nine hot springs; a temperature above 100°C was inferred from geothermometry indicators for some. Rubabo, Minera, Birara and Ihimbo were found to be promising (Bahati, 1995, 1996). Ármannsson (2001) visited Karungu, Minera, Ihimbo and Kitagata with the Geological Survey and Mines geochemical team and found them promising. The preliminary investigation was started again in 2005 under a project of the government of Uganda with support from the World Bank (WB) and the Icelandic International Development Agency (ICEIDA) with the aim of ranking geothermal areas outside tectonic and volcanic areas of Uganda for geothermal potential. Thirty two geothermal springs were initially considered, but subsurface temperatures could only be predicted with certainty for eight of them. Based on permeability and subsurface temperature, the most promising springs included Rubaare (134-140°C), Kitagata (120-140°C), Kanangorok (140-160°C), Ihimbo (80-100°C), Panyamur (80-120°C), Birara (140-160°C), Minera (120-130°C) and Rubabo (120-140°C). However, the presence of H_2S in Ihimbo and Panyamur may be an indication that the temperature may be higher than predicted. Other areas included Amuru, Kabuga, Kibenge, and Kaitabosi. These samples also had high magnesium concentrations that may be due to mixing with cold groundwater. All the samples had pH ranging from 6.84 to 10.55, and were low in trace elements. The main anion of more than half of the samples was sulphate even though the pH was high which is not common although it is similar in Katwe and Buranga. There were only two hot springs (Okumu and Amoropii) in which chloride was the main ion. Hydrogen and oxygen isotope studies showed that all the samples had deuterium excess (which could mean that the meteoric line for Entebbe does not apply). No oxygen isotope shift was observed for the samples (Ármannsson et al., 2008).

3. METHODOLOGY

The methods described below were used to study the chemistry of the hot springs to establish whether correlations between different springs existed.

3.1 Classification of geothermal waters using the Cl-SO_4-HCO_3 ternary diagram

Different chemical composition of geothermal water affects geothermometers in different ways; hence, classification gives an idea of the reliability of different geothermometers in each case. This is established in terms of major anions which are Cl^-, SO_4^{-2} and HCO_3^- (Giggenbach, 1991). The three well-characterised groups of waters include: highly acidic sulphate waters that can be formed as a result of the absorption of magmatic gases in groundwater; spring waters with carbon dioxide that are likely to represent waters with high carbon dioxide concentrations at the peripheries of hydrothermal systems; and discharge from geothermal wells associated with neutral chloride springs, likely to represent well equilibrated fluids from major upflow zones (Giggenbach, 1991). This differentiation is shown using the Cl-SO_4-HCO_3 ternary diagram. The positions of the data points on the ternary diagram were obtained by adding up the concentrations (in mg/kg) to obtain the sum of the three anions:

$$S = C_{Cl} + C_{SO_4} + C_{HCO_3}$$

The percentages of Cl, SO_4 and HCO_3 that is "%-Cl, "%-SO_4" and "%-HCO_3" were calculated from the total concentration and the concentrations of the individual anions:

$$"\%-Cl" = 100\, C_{CL}/S$$

$$"\%-SO_4" = 100\, C_{SO_4}/S$$

$$"\%-HCO_3" = 100 C_{HCO_3}/S$$

A work sheet was prepared using the Grapher program in percentages, with %-Cl listed in column A, %-SO_4 in column B, and %-HCO_3 in column C; column D represents: D = C + 0.5×A. Based on that a ternary diagram was plotted.

3.2 The Na-K-Mg diagram

A ternary diagram using Na, K and Mg concentrations was also plotted. This triangular diagram is used to classify waters into fully equilibrated, partially equilibrated and immature waters for the application of ionic geothermometers. These geothermometers work well with fully equilibrated waters. They are based on the temperature dependence of the following two reactions:

$$K\text{-}feldspar + Na^+ = Na\text{-}feldspar + K^+$$

$$2.8\, K-feldspar + 1.6\, water + Mg^{2+} = 0.8\, K-mica + 0.2\, chlorite + 5.4\, silica + 2K^+$$

From the following two geothermometers are derived:

$$t_{kn} = 933/(0.993 - L_{kn}) - 273.15$$

$$t_{km} = 4410/(1.75 - L_{km}) - 273.15$$

where $L_{kn} = \log(C_K/C_{Na})$ and $L_{km} = \log\left(C_K^2/C_{Mg}\right)$ and C is in mg/kg.

The square root of Mg is used because Mg^{+2} is a divalent ion. Therefore, two Na^+ or K^+ ions are needed in an exchange reaction with a Mg ion. The position of a data point in this triangular plot is first obtained by calculating the sum (S) of the concentrations C_i (in mg/kg) of all three cations, where:

$$S = C_{Na}/1000 + C_K/100 + \sqrt{C_{Mg}}$$

and

$$"\% - Na/1000" = C_{Na}/10S$$

$$"\% - K/100" = C_K/S$$

$$"\% - \sqrt{Mg}" = 100\sqrt{C_{Mg}}/S$$

Then, a worksheet is prepared with: *%-Na/*1000 in column A, *%- K/*100 in column B and *%-*$\sqrt{Mg}$ in column C and $D = C + 0.5^{*}A$ in column D. A ternary diagram can then be plotted with column A as the Y-axis and D as the X- axis. If a sample plots as immature water, then the application of Na-K and K-Mg geothermometers is doubtful while one plotting on the full equilibrium line suggests that water rock equilibrium is attained even at low temperatures (Giggenbach, 1991).

3.3 Classification of geothermal waters using the Cl-Li-B diagram

Giggenbach (1991) noted that the alkali metal Li is not affected by secondary processes and can, therefore, be used as a tracer for deep rock dissolution processes as a reference to evaluate the possible origin of the water. Cl and B, which are the most conservative constituents of geothermal thermal water, can be used in a similar way. The position of a data point in a triangular plot is obtained by calculating the sum of the concentrations *Ci* (in mg/kg) of all three:

$$S = C_{Cl/100} + C_{Li} + C_{B/4}$$

The percentages of Cl, Li and B/4 are calculated, that is *"%-Cl/100*, *"%-Li*" and *"%-B/4*", using the sum and concentrations of individual elements or ions as follows:

$$"\% - Cl/100" = C_{Cl}/S$$

$$"\% - Li" = 100\, C_{Li}/S$$

$$"\% - B/4" = 100\, C_{B/4}/S$$

A worksheet is prepared in Grapher, with "%-Cl/100" in column A, "% -Li" in column B, "%- B/4" in column C; in column D, $D = C + 0.5^{*}A$. A ternary diagram can hence be plotted.

3.4 Geothermometers

Geothermometers are used to predict subsurface temperatures in geothermal systems. These geothermometers used here are all based on the assumption that specific temperature-dependent mineral-solution equilibria are attained in the geothermal reservoir (Tole et al., 1993). The various geothermometers gave variable values for most of the geothermal fields. This may be due to a lack of equilibration with particular minerals, different rates of equilibration reaction between minerals and water, mixing with cold groundwater or boiling and condensation during upflow. Inferred subsurface temperatures of the geothermal hot springs were compared to find out possible temperature relationships between them. The geothermometers described below were used.

3.4.1 Silica geothermometers

The solubility of the silica minerals depends on temperature; it decreases significantly at temperatures below 340°C. However, at temperatures below 300°C and at a depth attained by commercial drilling for geothermal resources, variation in hydrostatic pressure has little effect on the solubilities of quartz

and amorphous silica (Fournier and Potter, 1982). Salt has a significant effect only at concentrations greater than 2-3 wt% (Fournier, 1985; Fournier and Marshall, 1983), however, small changes in pressure and salinity have greater effects at temperatures above 300°C. The solubility of silica is also affected by changes in pH. Water rock interactions fix the pH of reservoir fluids at between 5.0 and 7.5. Hence, dissolved silica in hydrothermal solutions can be used with near neutral pH. It is one of the most reliable geothermometers for waters with known steam fractions when this has been corrected for (Fournier, 1991). Equations 1-6 are different expressions for the quartz geothermometer. Temperatures in the range 20-250°C can be calculated. *S* is the concentration of silica in mg/kg:

Quartz:

$$t°\mathrm{C} = \frac{1309}{5.19 - \log S} - 273.15 \quad (1)$$

Quartz after adiabatic boiling to 100°C:

$$t°\mathrm{C} = \frac{1522}{5.75 - \log S} - 273.15 \quad (2)$$

Studies have shown that most of the silica which crystallises at the earth's surface is a mixture of quartz and moganite. The increased solubilities of chalcedony and chert were at first thought to be a result of their high surface to volume ratios. However, recent studies suggest moganite may be responsible for the solubility behaviour of these silica species. The apparent dissolution and precipitation rate of quartz/moganite increases exponentially with increasing moganite content due to the enormous surface area of a moganite-rich moganite/quartz mixture (Gíslason et al., 1997). Chalcedony and chert are intimate mixtures of quartz and moganite. Recent caloric studies (Petrovic et al., 1996) show that moganite is less stable than quartz, resulting in greater solubility of moganite than quartz. The moganite is depleted in weathered chert and chalcedony (Heaney and Post, 1992) and scarce in rocks older than 100 thousand years (Heaney, 1995). Experimental results (Fournier and Rowe, 1966; Fournier, 1977) indicate that the solubility of chalcedony is greater than that of quartz at low temperatures but the difference in solubility decreases with increased temperature, becoming similar at 200°C. There is an ambiguity when using silica geothermometers to determine temperatures less than 200°C, simply because chalcedony appears to control dissolved silica in some places and quartz in others. Chalcedony controls solubility in areas where the temperature is below 120°C. However, in areas where the rock has been in contact with the fluid at a given temperature for a relatively long time, like in deep sedimentary basins or rocks older than 100 thousand years, quartz controls dissolved silica concentrations at temperatures as low as 100°C. In areas where temperature is higher than 120°C, quartz usually controls the solubility of silica in old hydrothermal systems:

Chalcedony:

$$t°\mathrm{C} = \frac{1032}{4.69 - log\ S} - 273.15 \quad (3)$$

The other polymorphs of silica used as geothermometers include cristobalite (α-cristobalite), opal-CT (β-cristobalite) and amorphous silica obeying Equations 4, 5, and 6, respectively:

α-cristobalite:

$$t°\mathrm{C} = \frac{1000}{4.78 - log\ S} - 273.15 \quad (4)$$

Opal–Ct (β-cristobalite)

$$t°C = \frac{781}{4.51 - \log S} - 273.15 \quad (5)$$

Amorphous silica:

$$t℃ = \frac{731}{4.52 - \log S} - 273.15 \quad (6)$$

The results discussed in this project were calculated using the above chalcedony and quartz silica geothermometers.

3.4.2 Cation geothermometers

Cation geothermometers depend on ion exchange reactions which are temperature dependent. The geothermometers used include the Na-K geothermometer, the Na-K-Ca geothermometer and the K-Mg geothermometer.

The Na-K geothermometer

The Na-K geothermometer uses a reaction that involves simultaneous equilibrium between Na^+ and K^+ in solution and pure albite and K-feldspar that is expressed by the following equation:

$$NaAlSi_3O_3 + K^+ = KAlSi_3O_3 + Na^+ \quad (7)$$

and with an equilibrium constant of:

$$K_{eq} = \frac{[Na^+]}{[K^+]}$$

K_{eq} is the equilibrium constant, feldspar and albite are almost pure minerals with activity of approximately one (D'Amore and Arnórsson, 2000; Fournier, 1991).

Equations 8-12 give different proposed equations for the Na-K cation geothermometer:

Truesdell, 1976:

$$t℃ = \frac{856}{0.857 + \log(Na/K)} - 273.15 \quad (8)$$

Fournier, 1983:

$$t℃ = \frac{1217}{1.483 + \log(Na/K)} - 273.15 \quad (9)$$

Arnórsson et al., 1983 (25-250°C):

$$t℃ = \frac{933}{0.993 + \log(Na/K)} - 273.15 \quad (10)$$

Arnórsson et al., 1983 (250-350°C):

$$t℃ = \frac{1319}{1.66 + \log(Na/K)} - 273.15 \quad (11)$$

Giggenbach, 19883:

$$t℃ = \frac{1390}{1.50 + \log(Na/K)} - 273.5 \quad (12)$$

The Na-K-Ca geothermometer

This geothermometer is based on the exchange reaction between Na^+, K^+, and Ca^{+2} with mineral solids. The following equation has been proposed for it:

Fournier and Truesdell, 1973:

$$t°\text{C} = \frac{1647}{\log\left({}^{Na}/_{K}\right) + \beta \log\left({}^{Ca^{0.5}}/_{Na}\right) + 2.24} - 273.15 \quad (13)$$

Concentrations are in mol/kg.
β = 4/3 for temperatures <100°C and 1/3 for temperatures >100°C and for $\log(\text{Ca}^{0.5}/\text{Na}) < 0$;
β = 1/3 for water equilibrating above 100°C and 4/3 for water equilibrating below 100°C.

The value β = 1/3 should be used when the temperature of water is less than 100°C when log Ca^{+2}/Na is negative with concentrations expressed in molality units. However, when the geothermometer is applied to waters in which the partial pressure of CO_2 in the aquifer is above 10^{-4} atm, a correction factor I is subtracted from the right hand side of Equation 13, where:

$$I = -1.36 - 0.253 \log P_{CO_2} \quad (14)$$

K-Mg geothermometer

Giggenbach (1988) proposed the following equation for a K-Mg geothermometer:

$$t°\text{C} = \frac{4410}{14.0 + \log\left({}^{K^2}/_{Mg}\right)} - 273.15 \quad (15)$$

3.5 Fluid mineral equilibria calculations

Geothermometers are based on the assumption that specific temperature dependent mineral/solute equilibria are attained in geothermal reservoirs. For a particular geothermometer this only involves a few of the chemical components usually analysed in geothermal water. When different geothermometers are applied to the same fluid, different geothermometer temperatures are in some cases obtained. This could be due to a lack of equilibrium between respective solutes and hydrothermal minerals or due to reactions or mixing with water during upflow causing modification of geothermal fluid chemical composition.

Reed and Spycher (1984) proposed that the best way to estimate reservoir temperature is to consider simultaneously the state of equilibrium between a specific solution and many hydrothermal minerals as a function of time. The equilibrium constant is affected by both temperature and pressure. However, the pressure in geothermal systems is in the range 0-200 bar and has little effect on the equilibrium constant. Equilibrium constants vary widely with minerals; therefore, the temperature of convergence for a group of minerals in a log (Q_m/K_m) vs. temperature plot will likely be the temperature of the geothermal reservoir. For a reaction:

$$\Delta G_m = +\Delta G°_{m,r} + RT \log Q_m / K_m \quad (16)$$

where K_m is the equilibrium constant, ΔG is free energy, and Q_m is the activity coefficient.

At equilibrium, $\Delta G_m = 0$ and hence $\frac{\Delta G^o{}_{m,r}}{RT} = -\log Q_m / K_m$. When $Q_m = K_m$ the log (Q_m/K_m) = 0 at equilibrium, hence the plot of log (Q_m/K_m) vs. temperature will give all the minerals in equilibrium converging to a value of zero at the same temperature which is the temperature of the geothermal reservoir. Q_m and K_m were calculated using the WATCH computer code (Arnórsson and Bjarnason, 1993; Bjarnason, 1994) and the resulting graphs were plotted.

3.6 Mixing models

The estimation of subsurface temperature using surface discharges is based on the idea that geothermal fluids can cool in upflow zones either by conductive cooling or by boiling due to depressurisation or both. The fluids can, however, cool by mixing with cold water that will in most cases dilute and change the composition of the original fluids. Mixing after boiling or conductive cooling can upset chemical equilibria between water and rock minerals, hence changing their composition after mixing with respect to reactive components. Also, the concentration of non-reactive components in mixed waters is determined by the concentration and relative portions that make up the mixture (Arnórsson, 2000a). The chemistry of geothermal waters is characterised by equilibrium with solutes and alteration minerals while the composition of cold water appears to be determined by the kinetics of the leaching processes. The mixed water will tend to acquire a composition that may be intermediate (Arnórsson, 1985). In such cases, a uni-variant geothermometer will not give the temperature of the subsurface original fluids and will be misleading. Mixing of geothermal water with local cold water can be detected by a linear relationship between δ^2H and $\delta^{18}O$ or the aqueous concentration of conservative elements (Arnórsson, 2000b). This is important as assuming mixing for geothermal fluids where there is no mixing will give results that are too high. If the measured temperature is at least 50°C lower than the calculated silica and Na-K-Ca geothermometer temperatures, and the silica (quartz or chalcedony) geothermometer temperature is considerably lower than the Na-K-Ca geothermometer temperature, then mixing is likely to have taken place. The flow rate should also be high to allow little conductive cooling in the upflow (Fournier, 1981).

Two mixing models were used to estimate the potential subsurface temperature of the hot water end member of possibly mixed waters from which springs were emerging**:** the silica carbonate mixing model and the silica enthalpy warm spring mixing model.

3.6.1 The silica-carbonate mixing model

This model is based on the relationship between the silica and total dissolved carbonate concentrations. It is based on the assumption that practically all silica in geothermal reservoirs waters occurs as H_4SiO_4, and practically all carbonate carbon as carbon dioxide (Arnórsson, 2000b). Arnórsson et al. (1983) found out that carbon dioxide concentrations in waters in geothermal reservoirs were only dependent on temperature and, hence, on the overall solute - mineral equilibria in the reservoirs. It is also assumed that at temperatures above 200°C, most of the dissolved carbonate is in the form of carbon dioxide and that the silica concentration in high temperature fluid is determined by quartz solubility. The boiling of hot water leads to a drastic reduction in its carbonate content while mixing without boiling will produce water with a high carbon dioxide - silica ratio relative to equilibrated waters due to the curvature of the silica/carbonate relationship. The model helps to estimate the temperature of hot water in the mixed component and distinguish between boiled and unboiled fluids (Arnórsson, 2000b; Arnórsson, 1985).

Equations 17 and 18 are used to draw a curve giving a relationship between H_4SiO_4 and carbon dioxide, CO_2:

Arnórsson, 2000b:

$$SiO_2 = -15.433 - 151.60/T - 2.977 \times 10^{-6} T^2 + 5.464 \log T \quad (17)$$

and

$$CO_2 = -1.09 - 3894.55/T + 2.532 \log T \quad (18)$$

SiO_2 and CO_2 concentrations are in millimoles while T is in Kelvin.

The concentrations are changed to ppm. The data points are then plotted and those which plot above the curve represent boiled water while those below represent unboiled or degassed waters. A line is drawn from a point representing the concentration of silica and carbonate in cold water to that representing unboiled mixed water. The line is extrapolated and its intersection with the curve gives a point with the concentration of silica and carbonate of the hot water component in the mixture.

3.6.2 The silica enthalpy mixing model

Here, the solubility curve of quartz is drawn using Equation 19 and the temperature is converted into enthalpy of liquid water using Equation 20, or from steam tables:

Arnórsson, 2000b:

$$t(°C) = -55.3 + 0.3659S - 5.3954 \times 10^{-4}S^{-2} + 5.5132 \times 10^{-7}S^{2} + 74.360 \log S \quad (19)$$

and

$$h_{liquid} = 35.93 + 3.3053t + 2.3838 \times 10^{-3}t + 7.1004 \exp(0.04t) \quad (20)$$

The line for quartz solubility for liquid remaining after maximum steam loss was also drawn using Equation 21:

Arnórsson, 2000b:

$$t°C = -66.9 + 0.1378S - 4.9727 \times 10^{-5}S^{2} + 1.0468 \times 10^{-8}S^{3} + 87.841 \log S \quad (21)$$

In Figure 7, point A represents the concentration and enthalpy of cold water (non-thermal) that is mixed with geothermal water while B represents the composition and enthalpy of the mixed water. The temperature of the geothermal component of the mixed water is obtained by drawing a line through A and B that is extrapolated to point C that gives the initial silica and enthalpy composition of the hot water component. The temperature is obtained from steam tables. Point D is the intersection between the mixing line and the enthalpy of water at 100°C and atmospheric pressure.

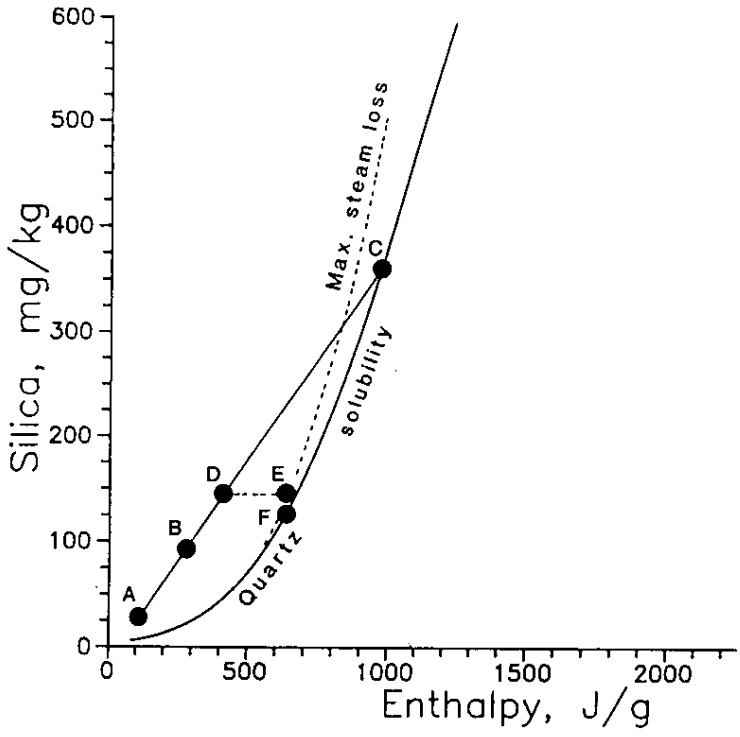

FIGURE 7: Enthalpy silica model for calculating silica mixing model temperatures

If the geothermal fluid boiled at atmospheric pressure before mixing, a horizontal line is drawn from D and the intersection of this line with the maximum steam loss curve then gives the initial enthalpy of the geothermal fluid (E). The initial dissolved silica before boiling and steam separation at atmospheric is represented by F which lies below E (Fournier, 1991).

4. SAMPLING AND ANALYSIS

The analytical results used in this project were obtained in 1993, 2002, 2003 and 2005**.** In 1993 in UNDP project (UGA/92/002), geological work was carried out in the Kibiro, Buranga and Katwe-Kikorongo geothermal areas. The samples were analysed at the Department of Geological Survey and Mines (pH, conductivity, CO_2, H_2S and NH_3) at Orkustofnun and the Science Institute of University of Iceland in Reykjavik. The details were discussed by Ármannsson (1994). The results from this project are numbered UG-93-X and UG-94-X where the number in the middle represents the year when the sample was analysed while X represents the sample number (Appendices, I, II, III and VI).

In 2005 in a project of the Government of Uganda with support from the World Bank and the International Development Bank, geochemical investigation involving the sampling of hot springs was carried out. The samples, which include water and rock samples, were analysed at the Institute of Geological and Nuclear Science New Zealand (Ármannsson et al., 2008). Results were obtained for the areas considered in this project which include Kabuga, Kibenge, Amuru, Amuru(Pakele) Avuka Amoropii, Kanangorok and Okumu. The samples analysed in this project include UG-O5- X where X represents 29 to 33, 58- to 68, 77, 80, 83, 117 and 118 (Appendices, IV and V).

Project UGA/8/003 (1999-2002) was renewed as Isotope Hydrology UGA/8/005 (2005-2006) with the objective of obtaining the origin of geothermal fluids, recharge mechanisms, resident times, predicting subsurface temperatures using isotope geothermometers and delineating the source of salinity and mixing processes. The work was carried out by International Atomic Energy Experts (IAEA) and Ugandan professionals. It involved sampling hot springs, groundwater boreholes and streams and was started in 1999. Hydrogen sulphide and carbon dioxide, temperature and conductivity were deterrmined in the field while environmental isotopes were determined by the IAEA Isotope Laboratory in Vienna (the results are presented in Appendices I to IV). In 2001 more samples were collected and analysed for isotopes in the IAEA laboratory Vienna, Institute of Hydrology (GSF) in Munich, Germany and the Institute of Geosciences and Earth Resources (CNR-IGG) in Pisa, Italy. In 2002, sampling was carried out in the Katwe and Buranga geothermal areas, constituting the last sampling campaign of the project. Similarly in 2005 in Kibiro, Buranga, with environmental isotopes analysed in the IAEA Isotope Laboratory in Vienna (presented in Appendices I to IV). The samples are numbered UG-99-X, UG-01-X and UG-05-X for samples analysed in different years under the project with X representing the sample number (Appendices I, II and IV). The other results used in this project were obtained by BGR and include samples UG-05-01 to UG-05-04 from Buranga hot springs and UG-05-06 to UG-05-08 from Kabuga, Kibenge and Rwagimba hot springs (Appendices I, II, VI).

5. RESULTS

5.1 Classification of geothermal waters

The Cl-SO_4-HCO_3 triangular plot was used for the classification of geothermal fluids with respect to the major anions Cl, SO_4 and HCO_3 (Figure 8). The Kibiro, Amoropii and Okumu samples plotted close to the chloride corner and were classified as mature neutral chloride waters. These likely formed from discharge from a geothermal reservoir associated with neutral chloride and represent equilibrated fluid from the upflow. Avuka and Amuru (Pakele) are peripheral bicarbonate waters, likely spring waters with high carbon dioxide at the periphery of the geothermal system. Kanangorok and Lake Kitagata plotted in the field of steam heated waters. Steam heated waters are usually formed as a result of absorption of magmatic gases into groundwater and are characterised by a low pH (Giggenbach, 1988). However, the hot spring fluids considered here are neutral to alkaline (Kanangorok 7.37, Lake Kitagata 8.03-8.61) and are likely to be volcanic fluids in which hydrogen sulphide has been oxidised to sulphate by processes other than oxidation by oxygen in groundwater.

Kabuga, Rwagimba, Kibenge and Lusoga borehole samples plotted as volcanic waters but the Amuru sample as bicarbonate water.

In the Cl-Li-B ternary plot, Li was used as a tracer for rock dissolution processes and for evaluating the possible origins of B and Cl. Kabuga, Kibenge, Rwagimba, Amoropii, Okumu, Lake Kitagata and Kibiro samples plotted close to the chloride corner indicating that these constituents originated in old hydrothermal systems (Figure 9). Due to either very low values of boron or lithium in the geothermal fluid samples (below detection limits), Amuru (Pakele), Amuru, and Kanangorok (apart from waters from the Kanangorok borehole) waters could not be plotted on the diagram. However, they contained almost 100% chloride and, therefore, would plot on the chloride vertex. The low values for lithium and boron may be an indication that the fluids come from old base rock rather than from the underlying sediments.

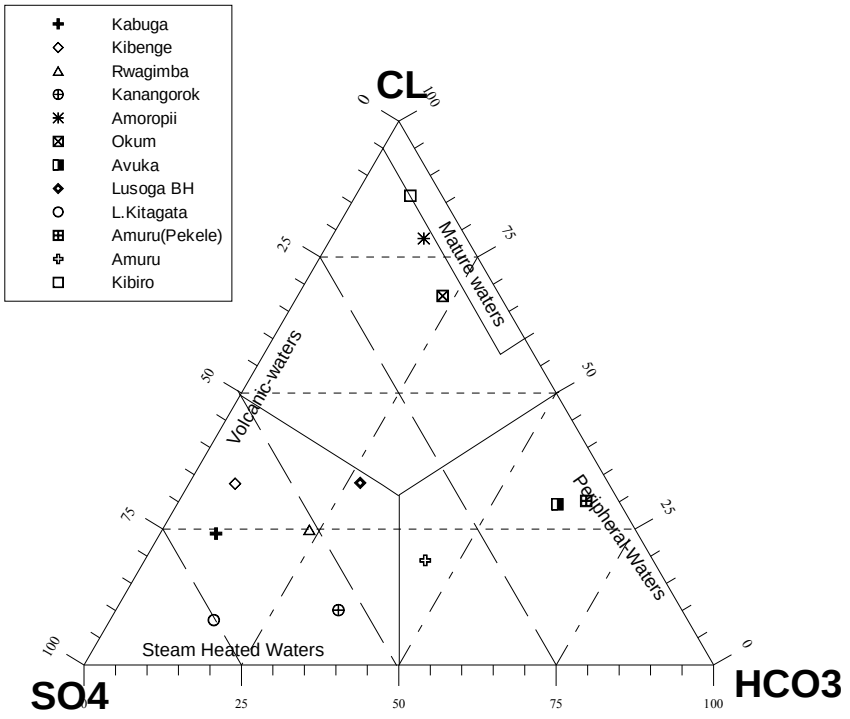

FIGURE 8: Classification of the geothermal waters using Cl-SO4-HCO_3 ternary diagram

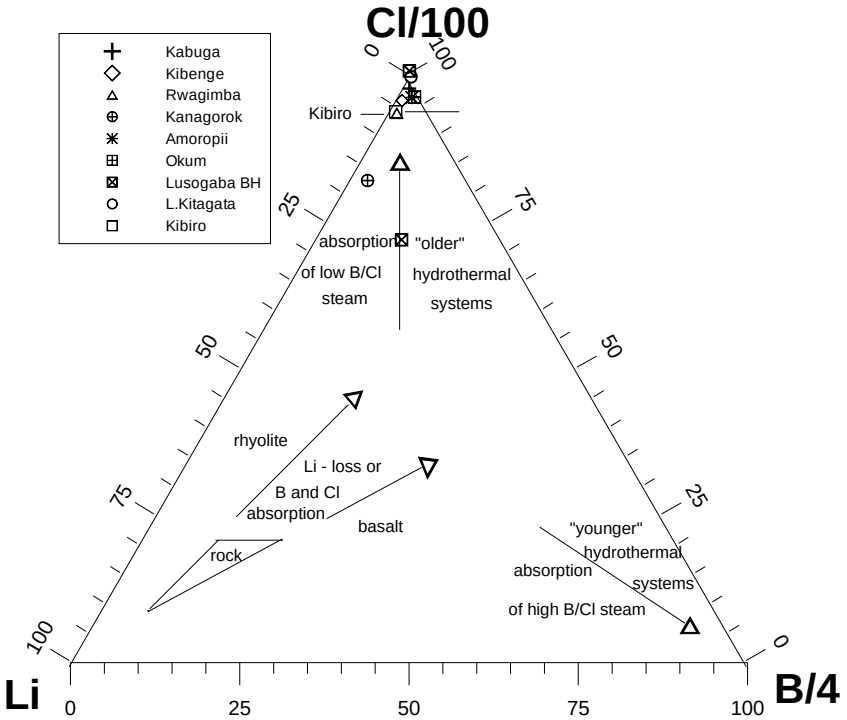

FIGURE 9: Classification of the geothermal waters using a Cl-Li-B ternary diagram

In the Na-K-Mg ternary plot, the geothermal fluids are classified as immature, partially equilibrated, and fully equilibrated waters. It shows which fluids are suitable for geothermometry, i.e. partially and fully equilibrated fluids. Kibiro, Rwagimba, Lake Kitagata, Kibenge, Kabuga, Amuru, Amuru (Pakele), Amoropii, Kanangorok, Avuka and Kaitabosi waters are fully or partially equilibrated (Figure 10a) and therefore can comfortably be used for cation geothermometry. The equilibrium curve is based on Icelandic basalt results (Arnórsson et al., 1983). Lake Kitagata and

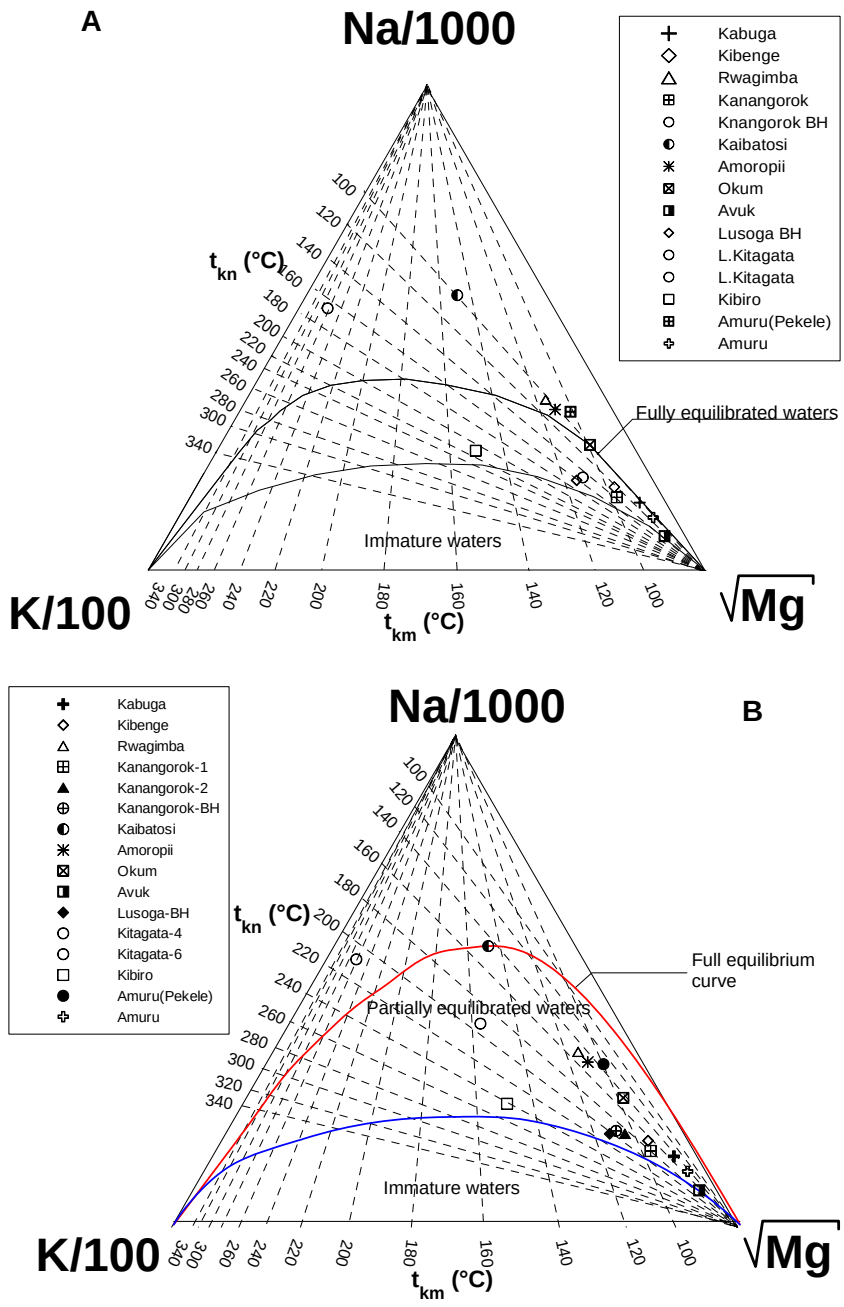

FIGURE 10: Classification of geothermal waters based on Na-K-Mg ternary diagrams, a) With the Arnórsson et al. (1983) equilibrium line; b) With the Giggenbach (1988) equilibrium line

Kaitabosi water samples plot above the equilibrium line. The reason could be that they derive from rocks that are not close in composition to the basalts used by Arnórsson et al. (1983). However, the Kaitabosi samples plot on the full equilibrium curve based on andesitic rocks (Giggenbach, 1988), while the Lake Kitagata water sample plots close to it (Figure 10b).

The Na-K-Mg ternary diagram was used to estimate the temperatures of the geothermal springs (Table 1) using Na/K and K/Mg geothermometers. There were some differences in the values for the two geothermometers. This could be due to the fact that when geothermal fluids ascend and cool without boiling there is a decrease in pH and temperature. This causes undersaturation with respect to primary igneous rocks which leads to more dissolution, lowering the ratio of K/Mg compared to Na/K in the rock. This leads to different values for Na-K and K-Mg geothermometers with K-Mg indicating a lower temperature (D'Amore and Arnórsson, 2000). The difference is also caused by the fact that the K/Mg geothermometer adjusts to changes in temperature faster than Na/K even for carbon dioxide rich waters. The K-Na geothermometer tends to preserve deep equilibrium values for Na/K ratios (Giggenbach, 1991).

TABLE 1: Temperature estimates for different hot springs based on the Na-K-Mg triangular diagram

	Kabuga	**Kibenge**	**Rwagimba**	**Kanangorok**	**Kaitabosi**	**Amoropii**	**Kitagata**	**Kibiro**
Na/K	130	130	108	150	100	105	170	210
K/Mg	90	60	115	110	150	110	260	150

5.2 Fluid mineral equilibria

The Cl-Li-B ternary diagram shows that the Okumu geothermal water is fully equilibrated and Kabuga, Amuru, Amoropii and Rwagimba waters plot close to the full equilibrium curve. It would be expected for these fluids to give a clear convergence of minerals that are believed to be in equilibrium. This may be a test to prove that the fluids are in equilibrium with respect to some minerals in the rocks but not others. Due to relatively low temperatures, it takes a long time for the fluid to reach equilibrium with solutes. Water that is far from equilibrium with hydrothermal minerals shows no convergence of minerals at any specific temperature. It distinguishes equilibrated geothermal fluids from those that have departed from equilibrium due to boiling or mixing with cold water.

The geothermometer temperatures below were estimated using the WATCH speciation programme (Table 2 and Figure 11). In some geothermal fluids of Kibenge, Kabuga and Okumu, the mineral curves intersect above the zero line giving a positive value of log (Q/K). This is possible if boiling takes place before sampling due to loss of vapour and gases leaving behind a residual solution with a simple non-volatile component (Arnórsson, 1985). However, this is not the case since the silica-carbonate mixing model indicates that there is no boiling in these hot springs. The Amuru curves intersect below the zero line giving a negative log (Q/K). This happens when the mixing of the fluid with dilute solutions lowers the log (Q/K) value. The Amoropii sample showed no clear convergence of mineral curves. The geothermal fluid could have mixed with fluids of different composition which interferes with its equilibrium. Also, if it mixes with fluid with solutes in a proportion very different from that of the geothermal fluid, there is a complete lack of any equilibrium (Figure 10). In the log (Q/K) versus temperature plots (Figure 11), only minerals expected to be in equilibrium were considered. Amorphous silica was not used as equilibrium was thought to be controlled by quartz or chalcedony. Also, because of dilute fluids mainly in northern Uganda hot springs, calcite and anhydrite were not used for locating points of intersection or equilibrium points as there was not enough calcium to saturate anhydrite and calcite. Few minerals were in equilibrium with the fluids. Due to the low temperature the interaction of the fluids takes a long time before equilibrium is attained. For Rwagimba and Kanangorok, geothermal temperatures estimated using WATCH were higher than the average measured temperature used in WATCH. The average measured temperature is the average of Quartz, chalcedony and Na/K geothermometer temperatures estimated using the WATCH computer code. Kabuga, Kibenge, Okumu and Amoropii waters show equilibrium at the chalcedony temperature while Rwagimba and Amuru waters show equilibrium at the quartz temperature. Kanangorok geothermometer temperatures were higher than the average measured temperature.

TABLE 2: Temperature estimated with WATCH and calculated temperature with geothermometers

Location	Sample no.	T_{WATCH} (°C)	Ionic balance (%)	Quartz temp. (°C)	Chalcedony temp. (°C)	Na/K temp. (°C)
Kabuga	UG-05-29	62-70	2.53	104.0	73.8	100.2
Kibenge	UG-05-30	67-73	2.97	97.5	66.8	121.6
Rwagimba	UG-05-33	118	0.35	114.3	85.0	93.1
Kanangorok-1	UG-05-58	157	2.85	138.4	111.6	139.4
Kanangorok-2	UG-05-59			145.0	119.0	146.0
Kanangorok-BH	UG-05-60			144.9	118.9	153.2
Kaitabosi	UG-05-61	-		26.9	-3.1	93.7
Amoropii	UG-05-62	?	-0.28	111.3	81.8	98.5
Okumu	UG-05-63	70-90	3.05	112.9	83.6	95.4
Avuka-2	UG-05-64	-	15.21	104.6	74.5	139.6
Amuru (Pakele)	UG-05-117		-17.76	78.7	46.7	82.5
Amuru	UG-05-118	100	-2.44	114.0	84.7	106.8

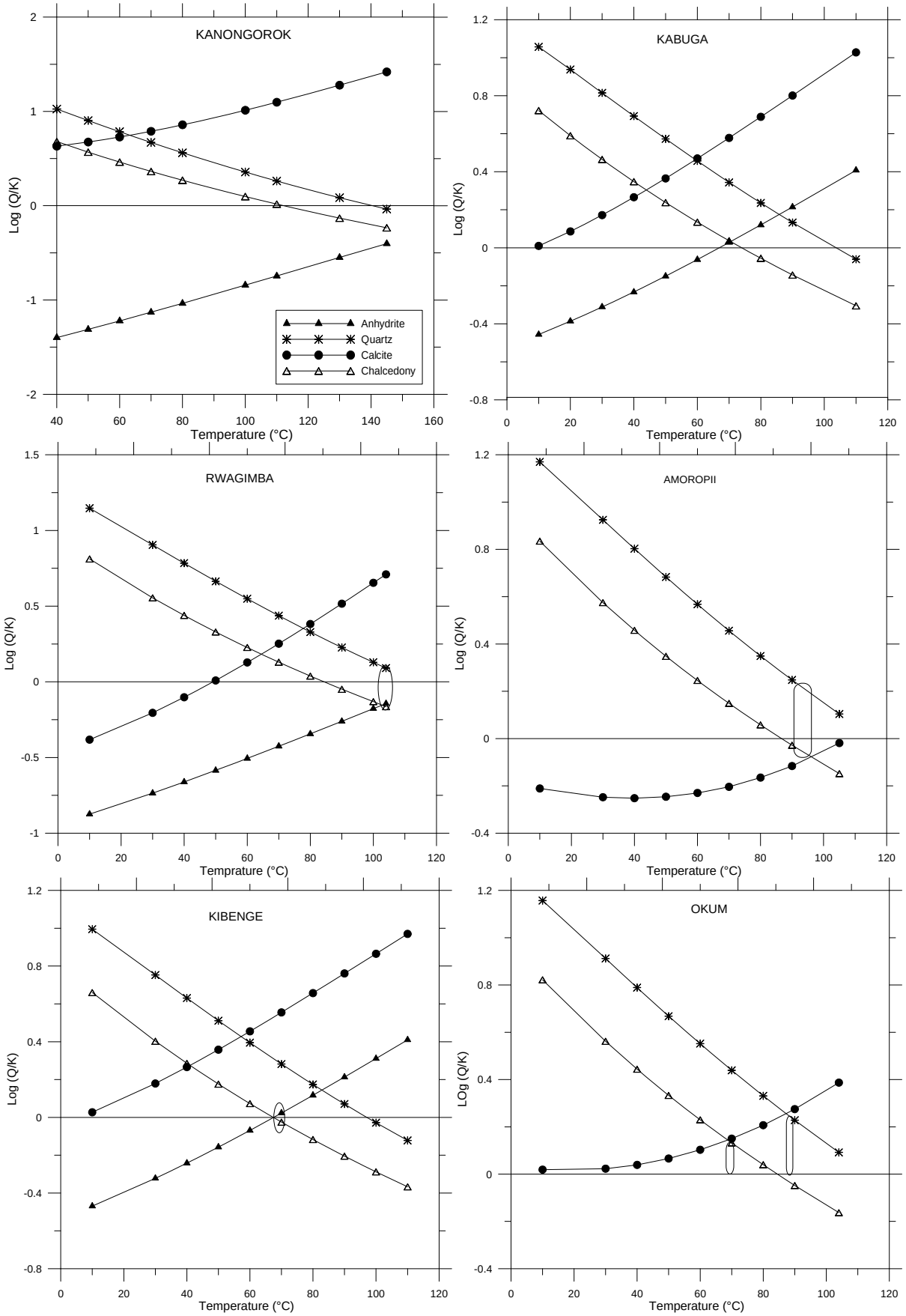

FIGURE 11: Saturation index diagrams of log Q/K versus temperature

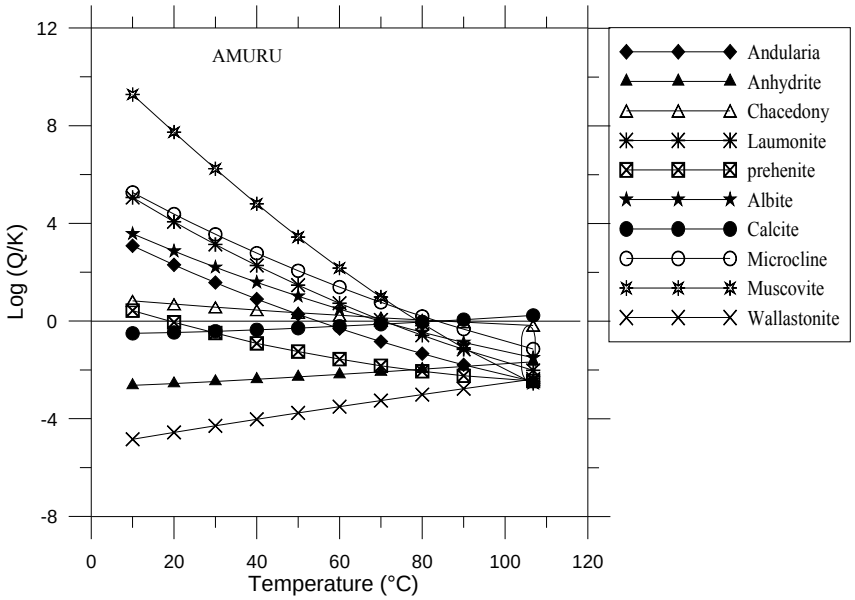

FIGURE 11 Cont.: Saturation index diagrams of log Q/K versus temperature

5.3 Kibiro, Panyamur, Amuru, Amuru (Pakele) and Kanangorok hot springs

Kibiro fluid flow is controlled by two intersecting faults, with the main one trending in a NE-SW direction and the other oblique to that. Panyamur springs (Avuka, Amoropii, and Okumu) lie along the escarpment of the rift valley and appear to be controlled by it. The altitude of Kibiro and Panyamur springs is not so different that it will stop the flow in either direction.

The isotope ratio plot (Figure 12) shows excess deuterium in Panyamur and other springs in northern Uganda. However, samples from Panyamur hot springs (Okumu, Amoropii and Lusoga BH) plot together with Kibiro groundwater and close to the Kibiro geothermal samples. The water samples plot on a line together with samples from other geothermal areas of Uganda apart from Katwe, Buranga and Kibiro. This, together with a small oxygen isotope shift, could mean high permeability and interaction of geothermal fluids with Kibiro groundwater. The plotting of Panyamur samples close to Kibiro samples may be an indication of correlation between the geothermal fluids of Kibiro and Panyamur hot springs.

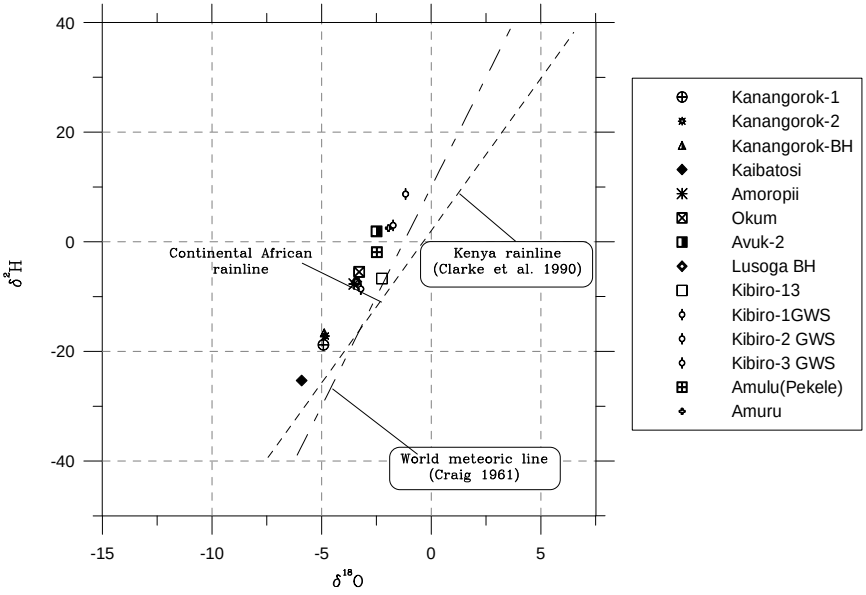

FIGURE 12: Isotope ratios of Kibiro and northern Uganda hot springs

The differences and similarities were further tested by studying conservative elements in the fluids from Kibiro (Mukabiga, Muntere and Mwibanda) and Panyamur. The conservative elements form soluble minerals and their supply is too limited to saturate the fluids (Arnórsson, 2000b). The concentrations can vary as a result of dilution but the ratio remains the same. The ratios considered include Cl/B, Cl/Li, Na/Cl and fluids of similar origin should have the same ratios.

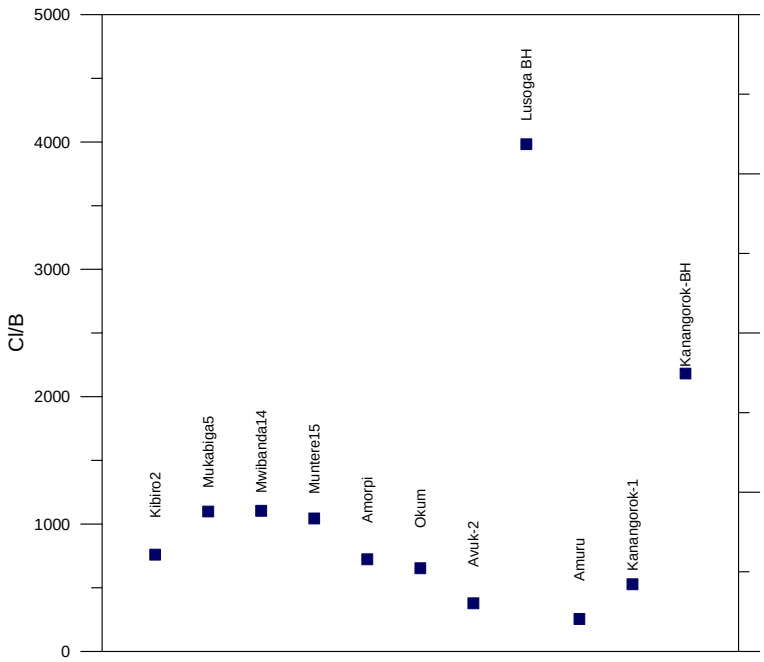

FIGURE 13: Cl/B ratio in Kibiro and northern Uganda hot springs

The Kibiro geothermal hot spring samples, which include samples from Mukabiga, Muntere and Mwibanda, have Cl/B ratios (Figure 13) ranging from 759 to 1104. This is not very different from Panyamur hot spring samples with a range of 653-723, despite being analysed in different years, while others outside the rift had very low values. However, the borehole samples have a high ratio due to high chloride values. The boron values for Amuru (Pakele) water were below the detection limit for boron so its Cl/B ratio could not be calculated. The Lusoga borehole contained groundwater while the Kanangorok BH sample is likely intermediate between groundwater and geothermal water (Appendix VIII). The Cl/B ratio plot shows Amoropii and Okumu samples plotting close to Kibiro samples (Figure 13) while Amuru and Kanangorok samples had considerably lower ratios except for the borehole samples. Amuru (Pakele) samples had a low boron concentration, below the detection limit (Appendix IX).

The concentration of boron is affected by both temperature and the permeability of rocks in reservoirs. Literature shows that Cl is incompatible in alteration phases in all natural water - rock environments whether at ambient or elevated temperatures. It is not adsorbed on a mineral surface (Hem, 1970), nor does it enter any common forming mineral, due to its large size. Also, when temperatures are high, B is mobile and incompatible as observed from many water - rock interaction experiments (Mahon and Ellis, 1970). However, at lower temperatures, below 100-150°C, experiments have shown that B is incorporated in secondary minerals (Arnórsson and Andrésdóttir, 1995). It is adsorbed and incorporated in clay minerals, mainly illite (Harder, 1970) and behaves as incompatible in geothermal systems above 150°C (Ellis and Mahon, 1964, 1967; Ellis, 1970). These could be the reasons for the lower values of B in Panyamur geothermal hot spring water where temperatures are as low as 84°C according to the geothermometers. B might, thus, have been scavenged from the solution. Even some samples that have no detectable concentrations like the Amuru (Pakele) sample could be the cause of a slight variation in Cl/B ratios compared to those of Kibiro.

The Cl/Li ratios are lower for Kibiro hot spring samples than the Panyamur ones (Okumu and Amoropii, Figure 14) The difference in Cl/Li could be attributed to very low values of lithium (Okumu 0.08 mg/kg) that might increase error in analysis.

Kibiro hot spring waters have a Na/Cl ratio close to that of Amoropii and Okumu water samples while the rest has a high ratio due to a small concentration of chloride (Figure 15). Okumu and Amoropii samples have the same range of Na/Cl ratios as the Kibiro geothermal fluid samples. From the Cl-SO_4-HCO_3 triangular diagram for the classification of geothermal fluids (Figure 8), Kibiro, Amoropii,

and Okumu waters are classified as mature chloride waters, while Amuru, Amuru (Pakele) and Amuru waters classify as bicarbonate peripheral waters. Another similarity between Kibiro, Amoropii, and Okumu water samples is that they all contained hydrogen sulphide and ammonia whereas the rest of the hot springs in northern Uganda did not have detectable concentrations of these constituents. However, there appears to be no clear temperature gradient between Kibiro, Okumu and Amoropii. This could be due to the short distance between Okumu and Amoropii. Kibiro had an estimated subsurface temperature of 200°C and its geothermal fluid had mixed with cold groundwater to give a subsurface temperature of about 150°C**.** The Okumu quartz temperature is 113.3, chalcedony temperature 83.6, and Na/K 95.4, while the Amoropii quartz temperature is 113.3, the chalcedony temperature 81.8, and the Na/K temperature 98.4.

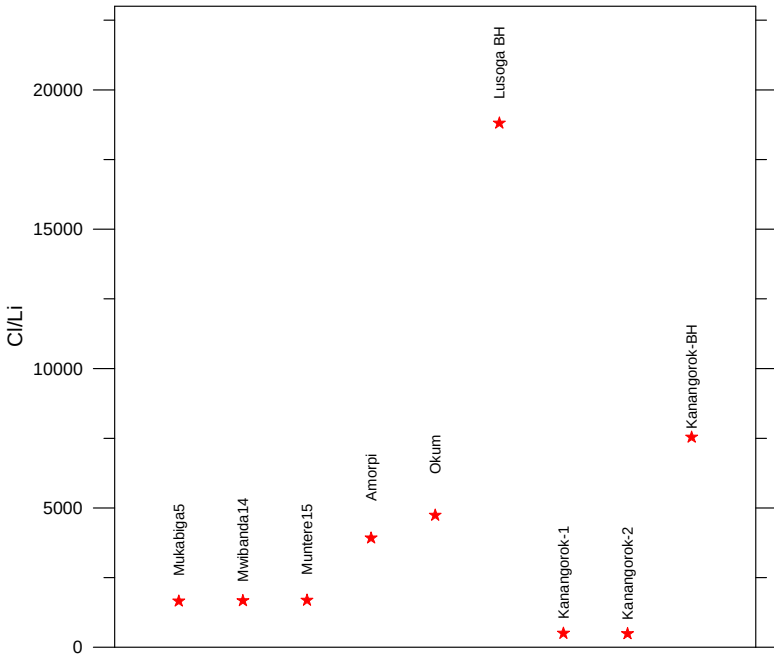

FIGURE 14: Cl/Li ratio in Kibiro and northern Uganda hot springs

A Na/K plot (Figure 16) shows that Kibiro water have low Na/K ratios and hence high temperatures while the Panyamur hot springs have high Na/K ratios, suggesting that they are low-temperature fluids. High temperatures tend to increase dissolution but give low Na/K ratios (Arnórsson, 1985).

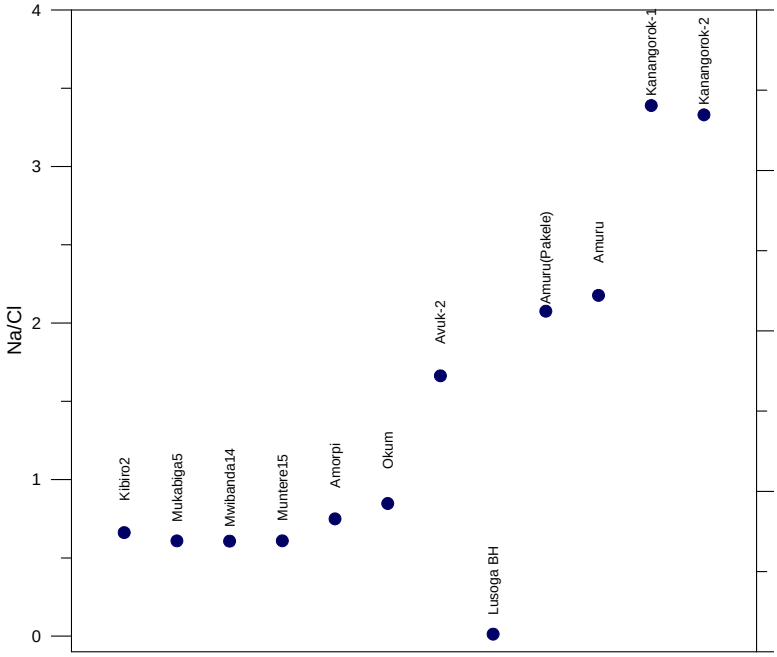

FIGURE 15: Na/Cl ratio in Kibiro and northern Uganda hot springs

Kanangorok 1 and Kibiro (Mwibanda, Mukabiga) waters have high concentrations of silica and high surface temperature compared to other hot springs (Figure 17). Kanangorok 2 and Kanangorok borehole waters have a low sampling temperature with relatively high silica concentrations. This, together with almost equal quartz and Na/K temperatures, shows that the low surface temperature is a result of conductive cooling rather than mixing with cold groundwater. Kanangorok and Kibiro waters have high concentrations of silica and high sampling temperatures compared to other hot springs (Figure 17). The low sampling temperature of Kanangorok with relatively high silica and almost equal quartz and Na/K temperatures (Table 2) shows that the low sampling temperature was a result of cooling rather than mixing with cold groundwater.

The plots of Cl vs. B, Cl vs. Li, and Cl vs. Na show a strong correlation between Kibiro, Okumu and Amoropii waters (Figure 18). The Panyamur and other northern Uganda hot springs have lower concentrations. The lower concentrations could be attributed to low temperature of the fluids which requires a long time to increase their concentrations through dissolution of rocks. The plots show that with distance away from Kibiro, the concentrations decrease.

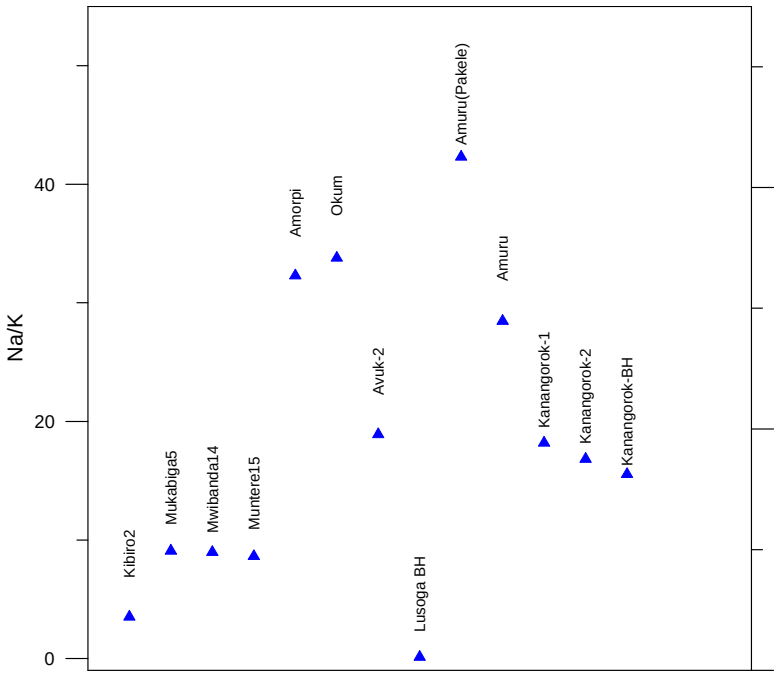

FIGURE 16: Na/K in Kibiro and northern Uganda hot springs

The results of the geochemical study shows that Kibiro waters are likely to be linked to Amoropii and Okumu waters. Carbon dioxide rich waters are also found at the boundaries of geothermal reservoirs in New Zealand (Hedenquist, 1990) and Olkaria geothermal field in Kenya (Arnórsson, 1991). Therefore, Avuka which is a part of Panyamur and is one of the Panyamur hot springs, is likely to be at the periphery of the 'Kibiro-Panyamur' geothermal field. This is also supported by the Cl-SO_4-HCO_3 diagram in which the Avuka water sample plotted as bicarbonate water (Figure 8).

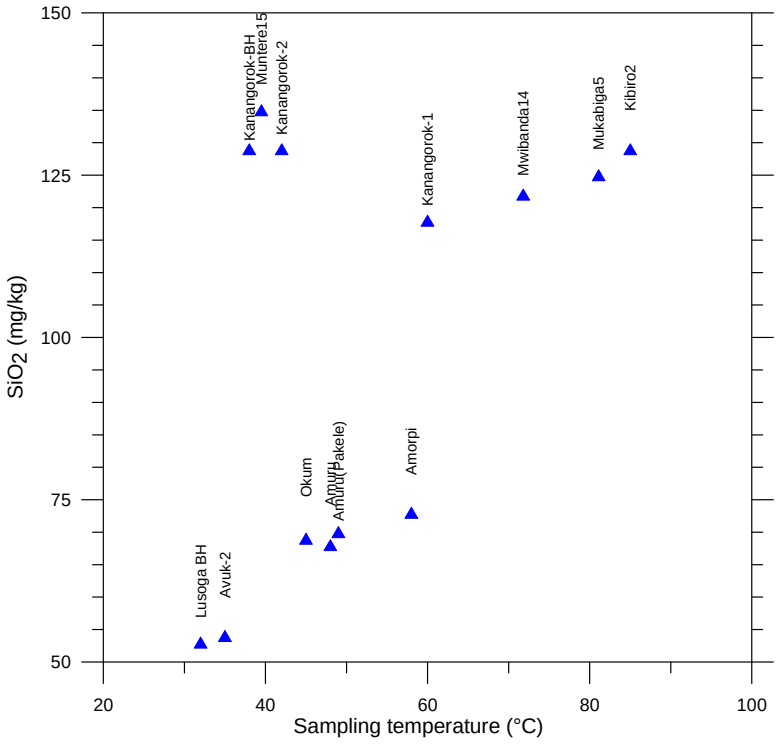

FIGURE 17: Variation of SiO_2 with surface temperature

5.3.1 Evidence of mixing

A positive correlation between the conservative elements and a linear relationship between them are typical of mixed waters (Figure 18). However, for a fluid to be considered mixed, there is likely to be a difference of about 50°C between the Na/K and quartz geothermometer temperatures (Fournier, 1981). Therefore, using this criterion of measured temperature compared to Na/K and quartz geothermometer temperatures, Avuka water (Quartz temperature, 104.6 and Na/K temperature 139.6) are considered to be mixed.

The Na-K-Mg ternary diagram is used to classify geothermal fluids into immature, partial and full equilibrium fluids (Giggenbach, 1991). Most of the hot spring samples (Kibiro, Kanangorok) plotted in the partial equilibrium region with only Avuka-2 plotting at the boundary of immature water and

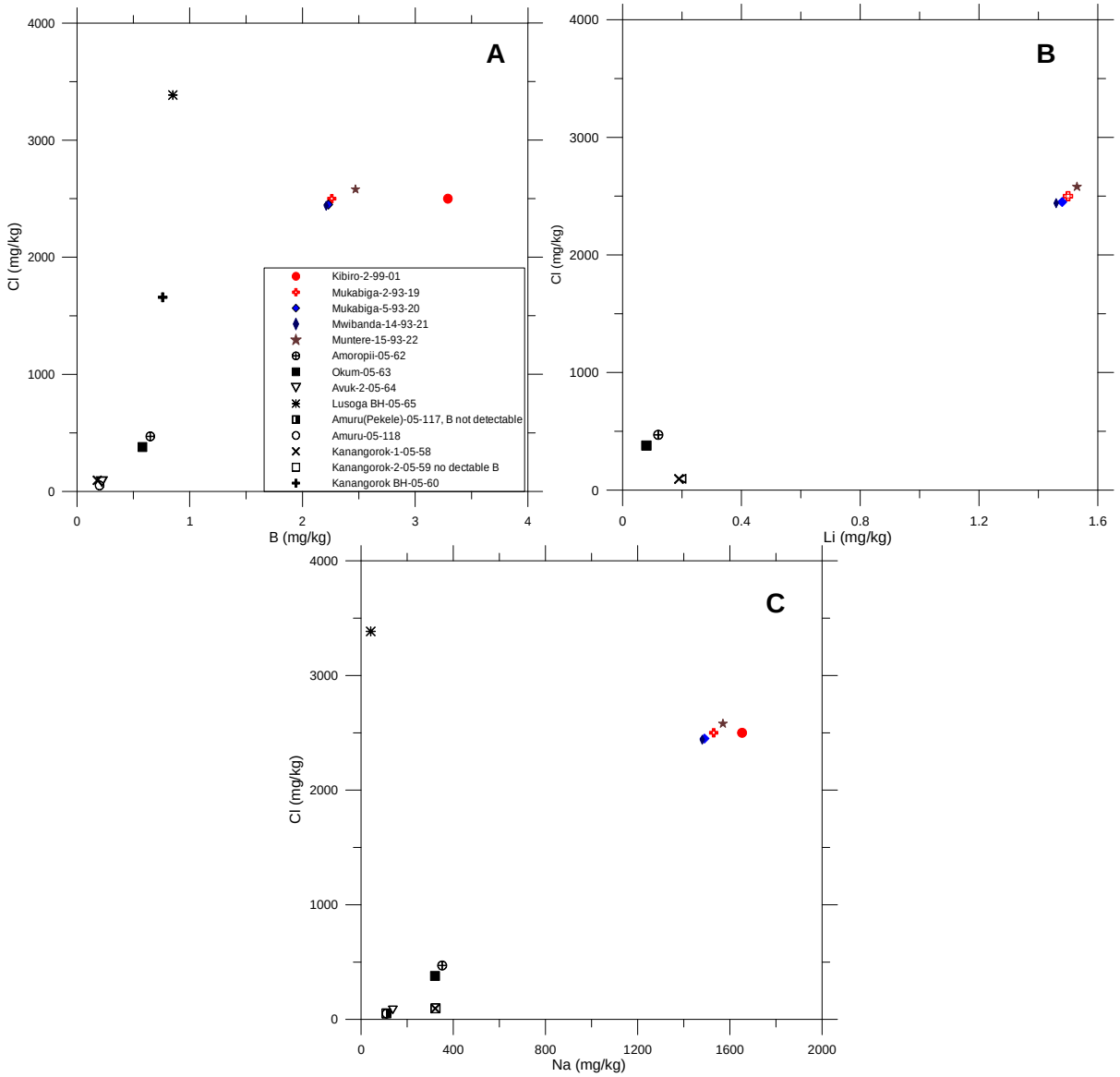

FIGURE 18: Graphs showing a) Cl vs. B, b) Cl vs. Li, and c) Cl vs. Na, in Kibiro and northern Uganda hot springs

partially equilibrated water. The log Q/K versus temperature diagrams for the samples which plotted close to equilibrium, Amoropii, Amuru, and Amuru (Pakele), did not show equilibrium with the minerals in the analysed geothermal samples (Okumu and Amoropii) at the expected temperatures. Lack of a clear intersection of saturation mineral curves could be due to mixing with either a solution of different composition or groundwater that was not dilute. Amuru and Kanangorok waters, whose curves intersected at a negative value for log Q/K, suggested mixing with dilute water.

Mixing also involves a lowering of Cl and B concentrations without effectively lowering the Cl/B ratio. The lowering of Cl and B concentrations of Amoropii and Okumu waters without too much lowering of the Cl/B ratio is also an indication of mixing. The mixed water is low in chloride relative to the water within the same reservoir which tends to be high in CO_2/H_2S (Okumu 44, Amoropii 12.7) while the ratio for Kibiro waters varies from 9 to 14. This could be due to reactions caused by mixing that tend to remove H_2 and H_2S from a solution relative to CO_2 (Hedenquist, 1990). The high value for the Okumu water might also be an indication of mixing.

HCO_3 is the major anion of Avuka, Amuru, and Amuru (Pakele) waters. Carbon dioxide may form by mixing of fluid that has not undergone fluid phase separation with cold groundwater (Arnórsson

1985). Carbon dioxide rich waters can also form by mixing mantle derived magmatic or metamorphic CO_2 with ground or surface waters (Arnórsson and Barnes, 1983).

The dissociation constant of carbonic acid increases with increasing temperature and thus the H^+ concentration increases. Mixed waters have a low pH with a high carbonic acid concentration. A pH of 6-7 for chloride concentrations less than 100 ppm is characteristic of mixed waters. Avuka water samples have a pH of 7.56 with a Cl concentration of 83 ppm. The increased H^+ concentration also causes rock dissolution that may lead to a drastic change in initial concentrations and approach the composition dictated by rock stoichiometric dissolution. This leads to an increase of Mg and Ca concentrations (mainly Mg) relative to the Na concentration (Arnórsson, 1991). Cooling by mixing affects exchange reactions with rock minerals and, thus, causes increases in the Na/K and Mg/Na ratios (Truesdell, 1991). The Mg/Na ratio for the Kibiro water varies from 0.002 to 0.006, in Kanangorok water it is 0.008, Amuru water 0.007 and Avuka water 0.022, which is the highest of the samples studied.

Geochemical isotope studies also show that Avuka appears to be recharged locally or has a component of lake water while the values for Okumu and Amoropii waters are lower, suggesting recharge from a higher altitude or mixing with local groundwater (Ármannsson et al., 2008). Therefore, the mixing model was only considered for Avuka, Okumu and Amoropii by taking account of gas ratios, log Q/K-temperature plots, and differences between quartz and Na/K temperatures. However the interpretation of Avuka and Amuru (Pakele) waters needs more work since the analyses yield poor ionic balances (Amuru (Pakele 11.9% and Avuka 15.12%) calculated by the WATCH speciation program.

5.4. Katwe-Kikorongo, Buranga, Rwagimba, Kibenge and Kabuga geothermal springs

Effort was made to study the geochemistry of the Katwe-Kikorongo, Buranga, Rwagimba, Kibenge and Kabuga geothermal springs to see if there was any possible correlation between them. For an isotope ratio plot, results from 1993, 1994, 2002 and 2005 were used. The plot of δ^2H versus $\delta^{18}O$ (Figure 19) shows that Buranga (including Kagoro), Kibenge, Kabuga samples could be grouped together and are different from those from the Katwe-Kikorongo field.

The results of plotting Cl versus B, Li and Na for Katwe-Kikorongo Kabuga and Rwagimba (Figure 20a-c) show that the 1993 results from the Kitagata-1 plot much higher on the graph than the rest and, once plotted with other results, the graphs display a pseudo correlation especially for the Cl/B and Cl/Na plots. However, when these points were removed, the other points are scattered (Figure 20d-f).

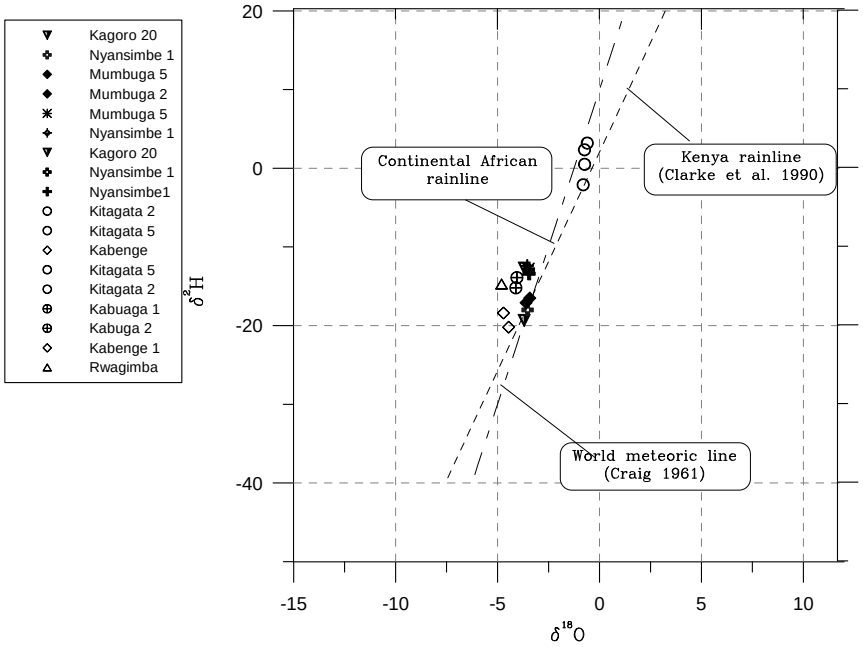

FIGURE 19: Variation of δ^2H with $\delta^{18}O$ for the Katwe-Kikorongo and Buranga geothermal fields

For Buranga, Kibenge, Kabuga, and Rwagimba the plots of Cl versus Na, Li and B show a strong

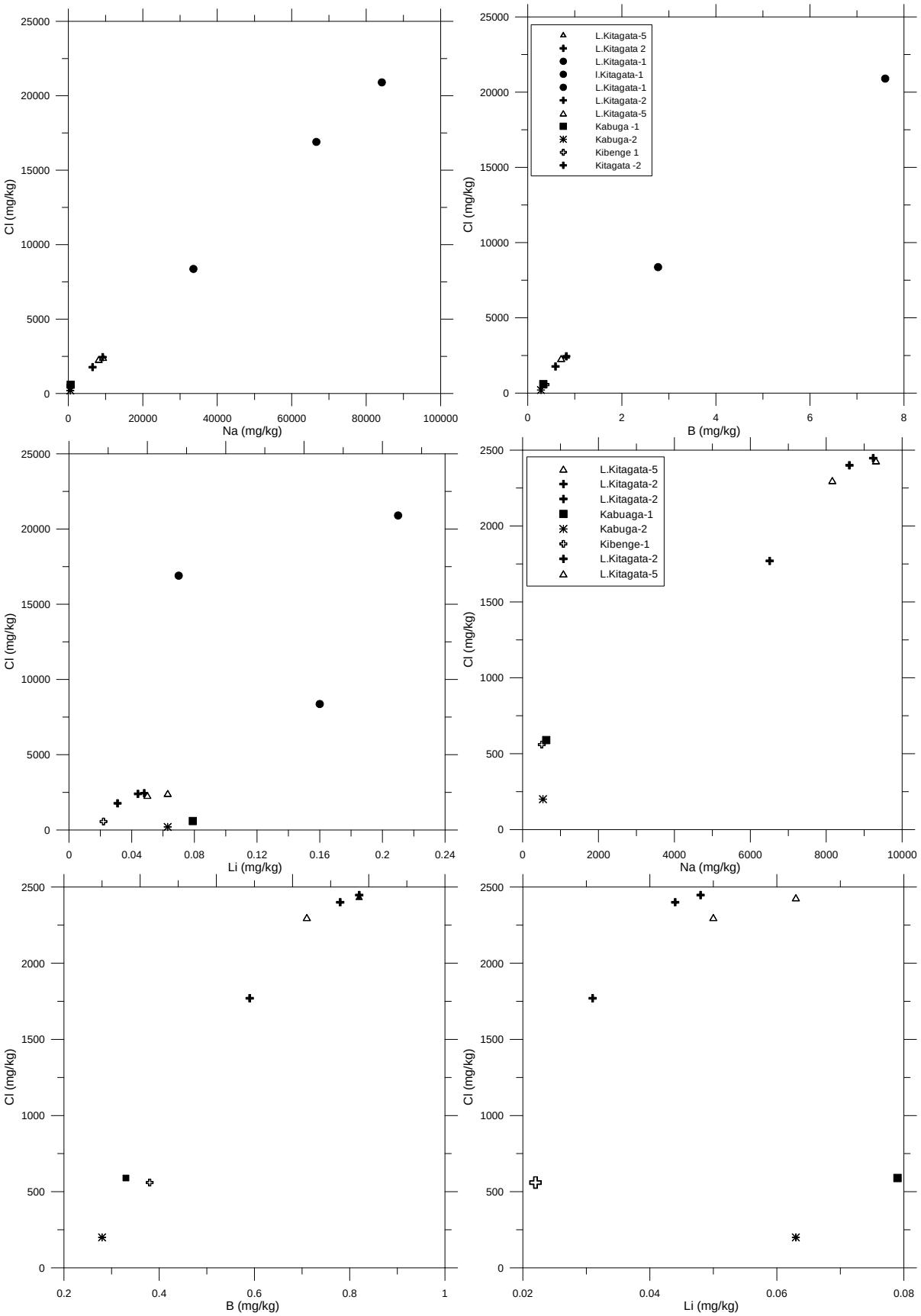

FIGURE 20: Variation of Li, B, and Na with Cl in Katwe-Kikorongo, Rwagimba, Kibenge and Kabuga hot springs; graphs a-c) include the Kitagata-1 1993 results, while graphs d-f) do not include these

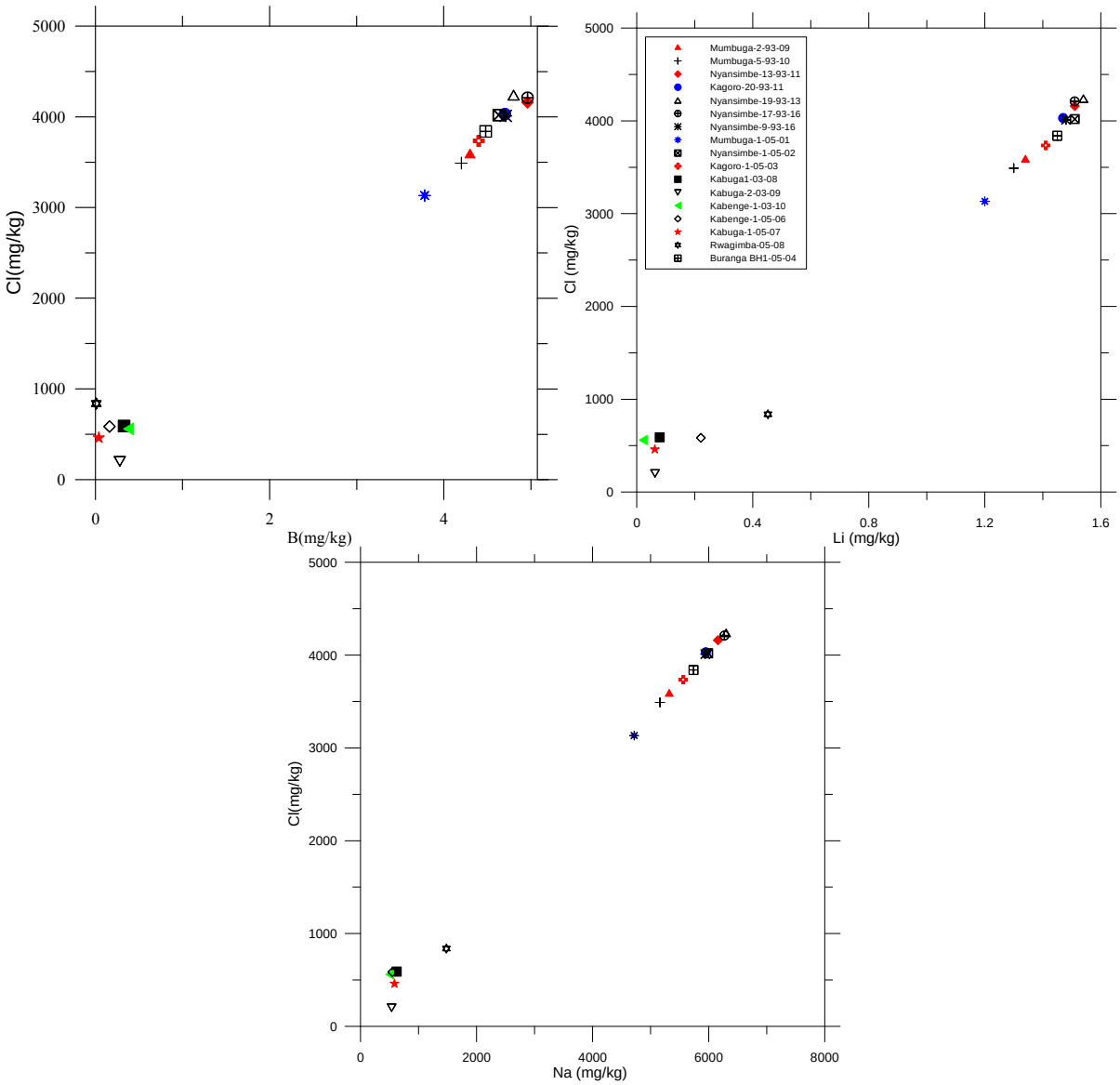

FIGURE 21: Variation of Cl vs. B, Li and Na in Buranga, Kibenge, Kabuga and Rwagimba hot springs

correlation (R^2 >0.995) between the conservative elements Cl, Li and B, indicating that the different hot springs are related (Figure 21). Kabuga, Kibenge and Rwagimba waters are more diluted than those of Buranga due to low temperatures and the long time needed for the fluids to interact with the rocks as seen earlier.

This grouping is also supported by different ratios between conservative elements. The ratios of different conservative elements from a geothermal fluid with a similar source of origin are constant or close despite changes in concentrations. The conservative element ratios studied include Cl/B, Cl/Li, and Na/K. Katwe-Kikorongo Cl/B values vary from 2963 to 2984, higher than Buranga ratios which varied from 831 to 868. The Kabuga-1 water's Cl/B ratio varies from 1788 in the 2003 analysis to 1277 in the 2005 analysis while Kabuga-2 water has a Cl/B ratio of 714, close to that of Buranga water. Kibenge values vary from 1219 to 1474 and the Rwagimba value is 1180, close to that of Buranga (Appendices VII and VIII).

A plot of the Cl/B ratios (Figure 22) shows the Buranga geothermal field samples plot close while the Katwe samples plot at high ratios. A Cl/Li ratio depicts a similar relationship (Figure 23). The Cl/Li ratio of Kibenge water (2647 analysed in 2005) is close to that of Buranga water (2611-2788) but

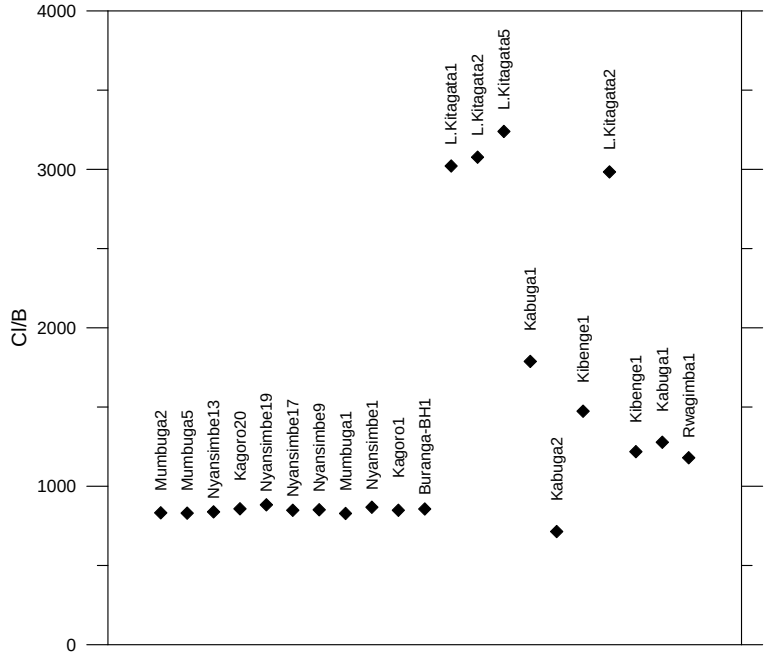

FIGURE 22: Cl/B ratio in Katwe-Kikorongo and Buranga hot springs

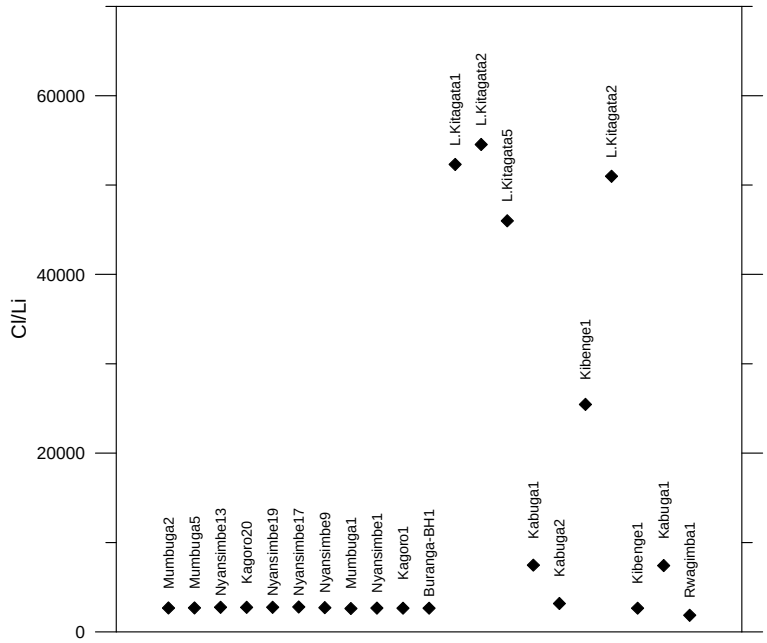

FIGURES 23: Cl/Li ratio in Katwe-Kikorongo and Buranga hot springs

much lower than the high ratios of Katwe waters (46,000-54,546). The plots show that Kibenge, Rwagimba and Kabuga and Buranga can be grouped together as one geothermal field.

The Buranga water Na/Cl ratio (Figure 24) varies from 1.48 to 1.51 while that of Lake Kitagata water varies from 3.5 to 4.0. The rest of the hot spring waters' ratios vary from 0.9 to 1.77, closer to Buranga than Lake Kitagata (Katwe-Kikorongo) water with Lake Kitagata water plotting above all other hot spring samples. The Na/K ratio for Buranga waters (Figure 25) varies from 26.7 to 27.8 in the 1993-2005 analyses which shows that they are consistent; Katwe waters register 11.8-19.0 in the 2003 analysis with an average of 15.98, Kabuga-1 water 21.2-24.9 (in the 2003 analysis) and 31.2 (in the 2005 analyses), Kibenge water give Na/K ratio of 18.7 according to the 2003 results, but 22.6 according to the 2005 analysis while Rwagimba water gives 35.6. Therefore, Kabuga and Kibenge waters correlate more closely to Buranga than Katwe waters. The results show that the Buranga hot springs (Nyansimbe and Mumbuga) and Rwenzori hot spring waters (like Kagoro) have Na/K ratios in the range 26.8 to 28.4 for the samples analysed in 1993-2005, thus showing consistency in the Na/K ratios (Appendix VII). The plot of Na/K ratios (Figure 25) shows this correlation although there are a few discrepancies which could be due to results obtained in different years. This shows that Katwe-Kikorongo geothermal field has higher temperatures than the Buranga geothermal field.

5.4.1 Evidence of mixing

The concentrations of many elements in the geothermal fluids of Katwe and Buranga are higher than those of the same elements in Kabuga and Kibenge fluids. This can also be said about the concentrations of Mg and Ca. This could be due to mixing with cold water and thus be the reason why their predicted subsurface temperatures are lower than those of the Buranga geothermal field. Magnesium in geothermal water rapidly decreases as temperature increases. However, as geothermal

fluids flow from a high-temperature environment to a low-temperature environment, they pick up relatively easily and quickly a significant amount of magnesium from rocks (Fournier, 1991). Therefore, the Kabuga, Kibenge and Rwagimba waters were considered for mixing models.

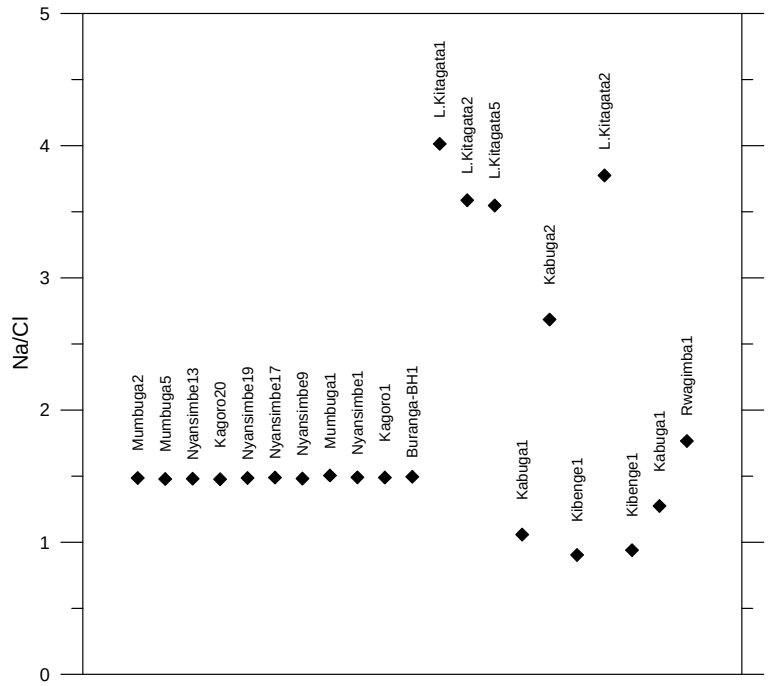

FIGURE 24: Variation of Na/Cl ratio of Katwe-Kikorongo and Buranga hot springs

5.5 Mixing models

Silica-carbonate mixing model temperatures

The silica-carbonate model was used to determine whether some of the fluids had boiled (Figure 26). The data plotted below the curve region representing unboiled or undegassed waters. It shows that Avuka, Amoropii, Kabuga, Kibenge, Rwagimba, Amuru and Amuru (Pakele) waters have never boiled.

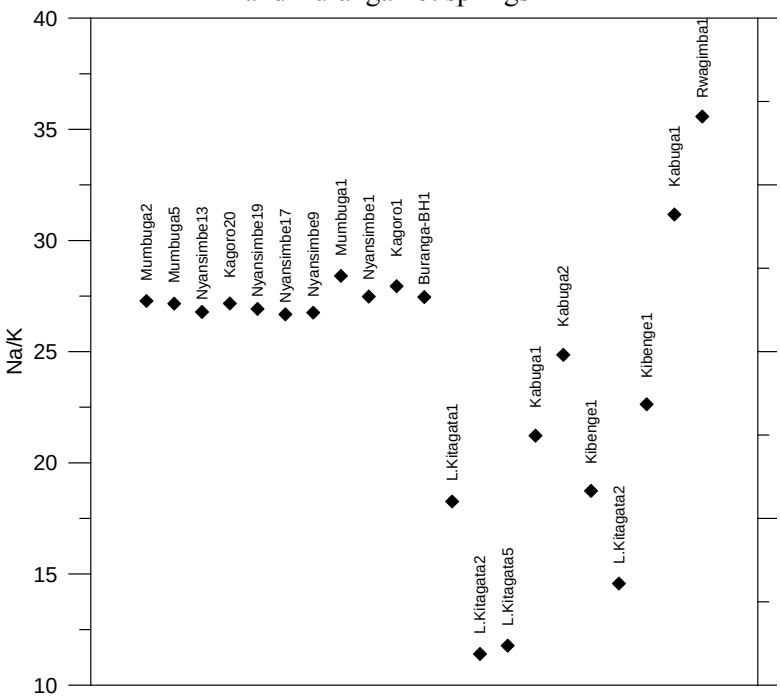

FIGURE 25: Variation of Na/K ratio of Katwe-Kikorongo and Buranga hot springs

Silica-enthalpy model for calculating silica mixing model temperatures

The silica concentration and the enthalpy of the unboiled samples were then plotted on a silica-enthalpy diagram together with the same parameters for a sample of cold water from the area (non-thermal water). A line was drawn joining the cold sample point to each of the hot spring sample points. The lines were extrapolated until they intersected the quartz solubility curve. The point of intersection represents the enthalpy and silica of geothermal water before mixing (Figure 27). The maximum steam loss curve was not used since the silica carbonate mixing model shows that there is no boiling. As can be seen in Table 3, the Kibenge and Rwagimba samples give a reading reasonably close to the temperatures for the Buranga samples. The rest of the samples give very high values and the extrapolated line for Avuka does not even intersect the solubility curve. This could be due to conductive cooling without loss of silica (for the case of non-boiling springs) that shifts data points to the left, giving a steep line or boiling (Arnórsson, 2000b). However, the boiling possibility has already been ruled out. The higher temperatures of other geothermal samples could be due to dissolution of silica after mixing as this leads to the estimation of high temperatures.

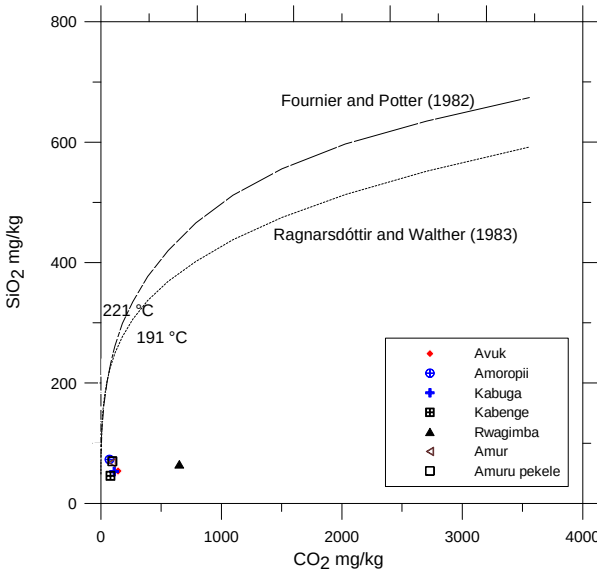

FIGURE 26: The silica-carbonate mixing model

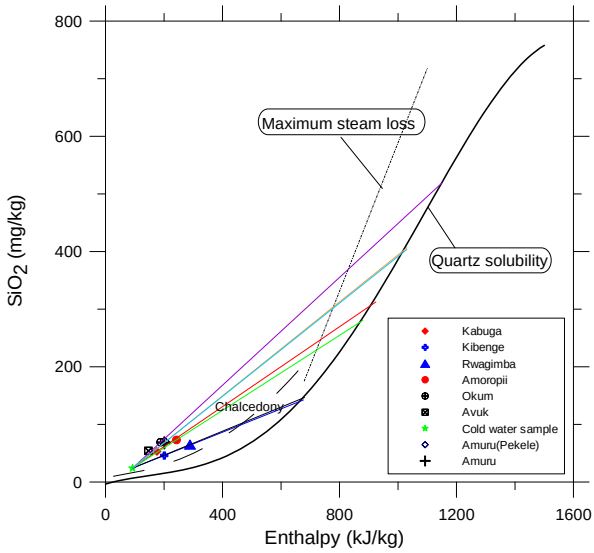

FIGURE 27: Silica-enthalpy mixing model for Buranga and northern Uganda hot spring samples

TABLE 3: Estimated temperature for some hot springs by the silica-enthalpy mixing model

	Kabuga	**Kibenge**	**Rwagimba**	**Amoropii**	**Okumu**	**Amuru (Pakele)**	**Amuru**
T(°C)	214	160.5	161	205	263	238	238

5.6 Scaling

The WATCH speciation programme was also used to predict scaling from the geothermal fluids studied. Using values for log Q and log K, plots of log Q against temperature were prepared with log K as the mineral used as a reference for the possibility of scaling. The values of log Q of the samples were plotted on the graph and those that plotted below the curve can be interpreted as undersaturated with no danger of scaling. The samples which plot above the curve in the supersaturated region suggest a danger of scaling upon utilisation, which needs further study. The results show that the fluids of Kanangorok, Kabuga, Rwagimba, Kibenge, Amoropii, Amuru and Amuru (Pakele) are undersaturated with respect to anhydrite (Figure 28a) and amorphous silica (Figure 28b). They were also undersaturated with respect to calcite, save for Kanangorok, Kabuga, Kibenge, Rwagimba, and Okumu (Figure 28c). The solubility of calcite decreases with increasing temperature with its value depending on the initial temperature and salinity of the geothermal water. It is high for high salinity and low temperature. The solubility of carbonate minerals in an aqueous solution at any particular temperature also increases with increasing partial pressure of carbon dioxide. Carbon dioxide has its minimum solubility in water at 160-180°C and carbon dioxide degassing at this temperature is most effective (Arnórsson, 1989). Pressure drop after partial phase separation can lead to extensive evaporation of flowing water. This causes an increase in ionic concentration and the degree of calcium carbonate supersaturation.

Cooling by boiling and increased aqueous silica concentrations (by steam loss) cause water to become supersaturated with respect to silica. Quartz precipitation is sluggish and silica is only removed from a solution at an appreciable rate if it becomes somewhat supersaturated with amorphous silica, particularly when supersaturated water comes into contact with air (Arnórsson, 1991). The temperature at which amorphous silica saturation is reached in wet-steam well waters depends on aquifer temperature and the pH of the water. Boiling causes the separation of water and steam phases in aquifers flowing towards the well (Arnórsson, 1981). Degassing of water of low salinity (less than 500 ppm) on boiling raises pH and thus causes silica dissolution. The ionised silica is not in

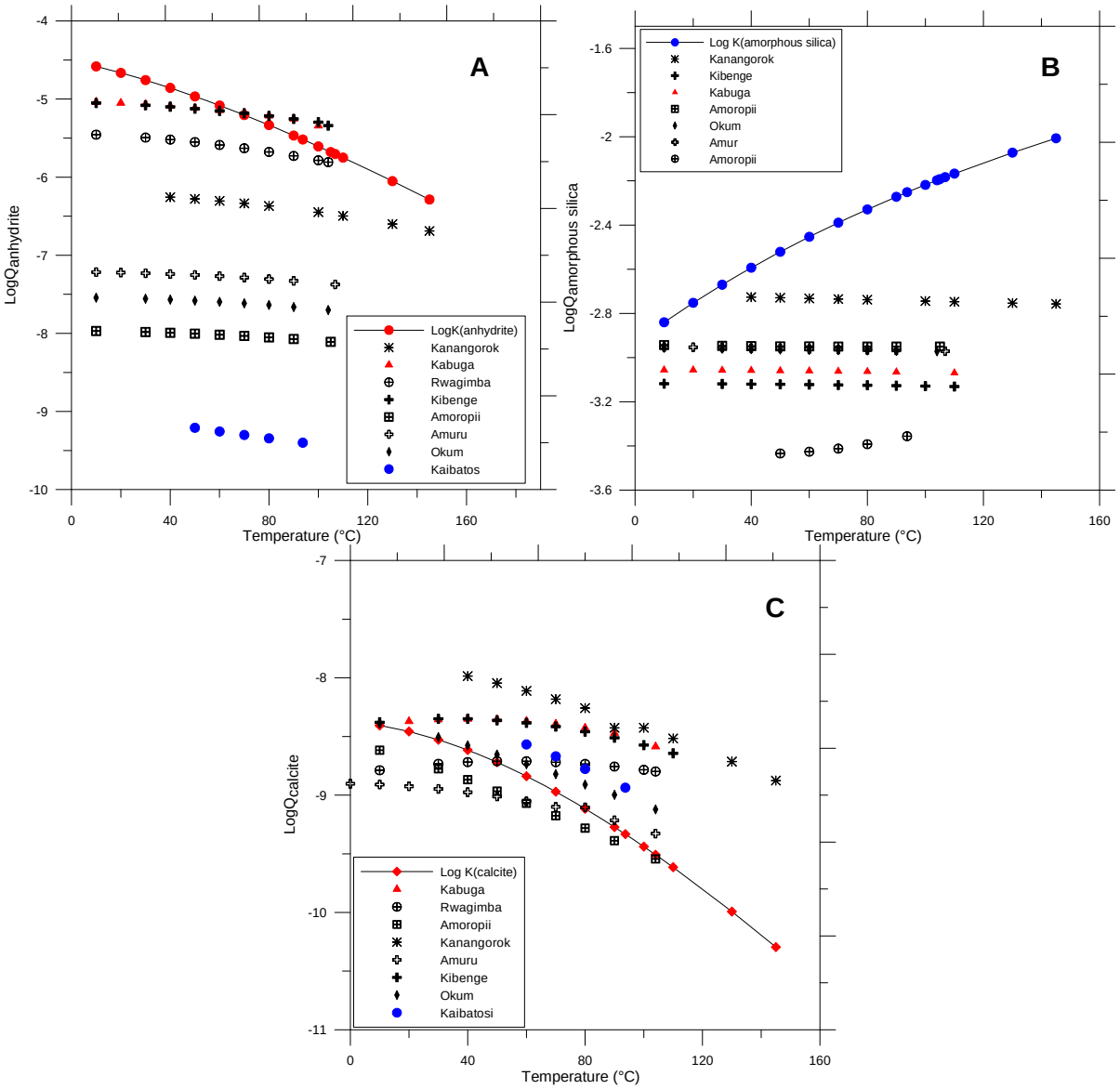

FIGURE 28: Variation of log Q with temperature for a) anhydrite; b) amorphous silica; and c) calcite

equilibrium with a solid phase and the ionisation of dissolved silica by pH rise lowers temperature at which amorphous silica saturation is reached (Arnórsson, 1991).

The rate of silica deposition is directly proportional to water temperature, the degree of water saturation and water salinity and inversely proportional to the extent of polymerisation of dissolved silica.

6. CONCLUSIONS

The main objective of the study was to find possible potential relationships between geothermal hot springs in Uganda. The major conclusions of the study include:

- The geochemical study of the geothermal fluids suggests that Kibenge, Kabuga, and Rwagimba are linked to Buranga and together these form one geothermal field.

- The Kibiro geothermal area is likely to be linked to Panyamur hot springs (Okumu, Amoropii, and Avuka) with Avuka likely to be at the periphery of the Kibiro-Panyamur geothermal field.
- Kabuga, Kibenge waters with measured temperatures of 100 and 126°C, respectively, are mixed with groundwater and the SiO_2-enthalpy mixing model indicates a reservoir temperature of 161°C.
- The geothermal waters studied rise from old hydrothermal systems rather than the young underlying sediments since they plot near the chloride corner on the Cl-Li-B ternary diagram.
- Comparing the Na-K-Mg ternary diagram with log (Q/K) versus temperature, the geothermal fluid concentrations are related to initial concentrations upon dissolution which are those dictated by the composition of the primary rock before any equilibrium is reached. Thus, the samples that plot as partially and fully equilibrated on the Na-K-Mg ternary diagram do not show clear convergence of mineral saturation curves.
- The silica-carbonate mixing model shows that there is no boiling in the Avuka, Amoropii, Kabuga, Kibenge, Rwagimba, and Amuru (Pakele) hot springs.
- The study shows a possibility of calcite scaling problems associated with the fluid utilisation from Kanangorok, Kabuga, Kibenge, Rwagimba, and Okumu hot springs.

The main recommendations are:

- More sampling should be carried out at Avuka and Amuru (Pakele) because of the poor ionic balance of the present samples which may reflect problems during sampling and analysis. The results for samples from these two hot springs may not be reliable.
- More detailed work should be carried out on Kibiro and Panyamur hot springs to confirm their link and a possible common geothermal source as the correlation obtained was based on a single analysis for each hot spring in Panyamur.

ACKNOWLEDGEMENTS

I would like to acknowledge BGR for supporting me in attending the UNU Geothermal Training programme for six months. I would also like to thank Dr. Ingvar Birgir Fridleifsson and Mr. Lúdvík S. Georgsson for giving me a chance to attend and the assistance given to me throughout the course. I would also like to extend my appreciation to Dr. Halldór Ármannsson, my supervisor, for professional guidance during the writing of the report. I would also like to thank the UNU fellows for the cordial relationship we had during the course.

I acknowledge the Ministry of Energy and Minerals, particularly the Department of Geological Survey and Mines, Uganda for allowing me to be away from my duty station for six months.

REFERENCES

Ármannsson, H., 1994: *Geothermal studies on three geothermal areas in West and Southwest Uganda.* UNDESD, UNDP project UGA/92/002, report, 85 pp.

Ármannsson, H. 2001: *Isotope hydrology for exploring geothermal resources. End of mission report*. IAEA Project UGA/8/003, report, 96 pp.

Ármannsson, H., Bahati, G., and Kato, V., 2008: *Preliminary investigation of geothermal areas in Uganda, other than Katwe-Kikorongo, Buranga and Kibiro.* DGSM, unpublished report.

Arnórsson, S., 1981: Mineral deposition from Icelandic geothermal waters, environmental and utilisation problems. *J. Petrol. technology*, *33,* 181-187.

Arnórsson, S., 1985: The use of mixing models and chemical geothermometers for estimating underground temperature in geothermal systems. *J. Volc. Geotherm. Res., 23,* 299-335.

Arnórsson, S., 1989: Deposition of calcium carbonate minerals from geothermal waters – theoretical considerations. *Geothermics, 18,* 33-39.

Arnórsson, S., 1991: Geochemistry and geothermal resources in Iceland, In: D´Amore, F. (co-ordinator), *Applications of geochemistry in geothermal reservoir development.* UNITAR/UNDP publication, Rome, 145-196.

Arnórsson, S., 2000a: Reactive and conservative components. In: Arnórsson, S. (ed.), *Isotopic and chemical techniques in geothermal exploration, development and use. Sampling methods, data handling, and interpretation*. International Atomic Energy Agency, Vienna, 200-211.

Arnórsson, S., 2000b: Mixing processes in upflow zones and mixing models. In: Arnórsson, S. (ed.), *Isotopic and chemical techniques in geothermal exploration, development and use. Sampling methods, data handling, and interpretation*. International Atomic Energy Agency, Vienna, 200-211.

Arnórsson, S., Andrésdóttir, A., 1995: Processes controlling the distribution of boron and chlorine in natural waters in Iceland. *Geochemi. Cosmochim. Acta, 59,* 4125-4146.

Arnórsson S, and Barnes I., 1983: The structure of carbon dioxide waters in Snaefellsnes, Western Iceland. *Geothermics 12,* 171-176.

Arnórsson, S., and Bjarnason, J.Ö., 1993: *Icelandic Water Chemistry Group presents the chemical speciation programme WATCH.* Science Institute, University of Iceland, Orkustofnun, Reykjavík, 7 pp.

Arnórsson, S., Gunnlaugsson, E., and Svavarsson, H., 1983: The chemistry of geothermal waters in Iceland III. Chemical geothermometry in geothermal investigations. *Geochim. Cosmochim. Acta, 47*, 567-577.

Bahati, G. 1995: *Preliminary geochemical investigations of Kitagata hot springs in Bushenyi District and Karungu, Bubale, Kagamba hot springs in Kabale District.* Geological Survey and Mines Department, Uganda, report No.GBB/7, 13 pp.

Bahati, G. 1996: *Preliminary geochemical investigations of Kisiizi, Minera, Rubabo, Birara, Ihimbo and Kiruruma hot springs in Rukungiri District*. The Geological Survey and Mines Department, Uganda, report No.GBB/12, 22 pp.

Bahati, G., 2007: *Isotope hydrology for exploring geothermal resources.* Dept. Geol. Surv. and Mines, Uganda, IAEA TC, project terminal report, UGA/8/005, 47 pp.

Bahati, G., and Natukunda, J.F., 2008: Status of geothermal exploration and development in Uganda. In: Georgsson, L.S., Holm, D.H., and Fridleifsson, I.B. (eds.), *Papers presented at "30th Anniversary Workshop of the United Nations University Geothermal Training Programme, Reykjavik*, CD, 10 pp.

Bahati, G., Pang Z. Ármannsson, H., Isabirye, E.M, and Kato, V., 2005: Hydrology and reservoir characteristics of three geothermal systems in western Uganda. *Geothermics, 34,* 568-591.

Bjarnason, J.Ö., 1994: *The speciation program WATCH, version 2.1.* Orkustofnun, Reykjavík, 7 pp.

D'Amore, F., and Arnórsson, S., 2000: Geothermometry. In: Arnórsson, S. (ed.), *Isotopic and chemical techniques in geothermal exploration, development and use. Sampling methods, data handling, interpretation*. International Atomic Energy Agency, Vienna, 152-199.

Ellis, A.J., 1970: Quantitative interpretation of chemical characteristics of hydrothermal systems. *Geothermics, 2,* 516-527.

Ellis, A.J., and Mahon, W.A.J., 1964: Natural hydrothermal systems and experimental hot water/rock interactions. *Geochim. Cosmochim. Acta, 28,* 1323-1357.

Ellis, A. J. and Mahon, W.A.J., 1967: Natural hydrothermal systems and experimental hot water/rock interactions. Part II. *Geochim. Cosmochim. Acta, 31,* 519-538.

Fournier, R.O., 1977: Chemical geothermometers and mixing models for geothermometers for geothermal systems, *Geothermics* 5, 41-50.

Fournier, R.O., 1981: Application of water chemistry to geothermal exploration and reservoir engineering. In: Rybach, L., and Muffler, L.J.P. (editors), *Geothermal system: Principles and case histories.* John Wiley and Sons Ltd., Chichester, 109-143.

Fournier, R.O., 1983: A method of calculating quartz solubilities in aqueous sodium chloride solutions. *Geochim. Cosmochim. Acta, 47,* 579-586.

Fournier, R.O., 1985: The behaviour of silica in hydrothermal solutions. *Rev. Econ. Geol, 2,* 45-61.

Fournier, R.O., 1991: Water geothermometers applied to geothermal energy. In: D'Amore, F., (coordinator), *Application of geochemistry in geothermal reservoir development*. UNITAR/UNDP publication, Rome, 37-69.

Fournier, R.O., and Marshall, W.L., 1983: Calculation of amorphous silica solubilities at 25^{o}C to 300^{o}C and apparent cation hydration numbers in aqueous salt solutions using the concept of effective density of water. *Geochim. Cosmochm. Acta, 47*, 587-596.

Fournier, R.O., and Potter, R.W. II, 1982: *An equation correlating the solubility of quartz in water from 25 to 900^{0}C at pressures up to 10,000 bars.* Geochem. Cosmochim. Acta, 46, 1969 -1974.

Fournier, R.O., and Rowe, J.J., 1966: Estimation of underground temperatures from the silica content of water from hot springs and steam wells. *Amer. J. Mineral*., 6, 459-464.

Fournier, R.O., and Truesdell, A.H. 1973: An empirical Na-K-Ca geothermometer for natural waters. *Geochim. Cosmochim. Acta*, 37, 1255-1275.

Giggenbach, W.F., 1988: Geothermal solute equilibria. Derivation of Na-K-Mg-Ca geoindicators. *Geochim. Cosmochm. Acta, 52*, 2749-2765.

Giggenbach, W.F., 1991: Chemical techniques in geothermal exploration. In: D'Amore, F. (coordinator), *Application of geochemistry in geothermal reservoir development*. UNITAR/UNDP publication, Rome, 119-142.

Gíslason, G., 1994: *Geothermal Exploration – I. UGA/92/002 & UGA/92E01: Terminal Report.* UNDDSMS – Geol. Surv. & Mines Dept., Uganda.

Gíslason, G., Árnason, K., Eysteinsson, H., 2004: *The Kibiro geothermal report*. *A report on geophysical and geological survey prepared for the Icelandic international Development Agency and the Ministry of Energy and Mineral Development, Uganda.* Unpublished report, 109 pp.

Gíslason, S.R., Heaney, P.J., Oelkers, E.H., and Schott, J., 1997: Kinetic and thermodynamic properties of moganite, a novel silica polymorph. *Geochim. Cosmochim. Acta, 61,* 1193-1204.

Harder, H., 1970: Boron content of sediments as a tool in facies analysis. Sediments analysis. *Sediment Geol., 4,* 153-175.

Heaney, P.J., 1995: Moganite as an indicator for vanished evaporates: A testament reborn? *J. Sediment. Res*. A65, 633-638.

Heaney, P.J., and Post, J.E., 1992: The widespread distribution of a novel silica polymorph in microcrystalline quartz varieties. *Science, 255*, 441-443.

Hedenquist, J.W., 1990: The thermal and geochemical structure of the Broadlands-Ohaaki geothermal system, New Zealand. *Geothermics*, *19,* 151-185.

Hem, J.D., 1970: Study and interpretation of the chemical characteristics of natural water. *U.S. Geol. Survey, water supply paper 1473.*

Henley, R.W., Ellis, A.J., 1983: Geothermal systems ancient and modern: a geochemical review. *Earth-Sci. Rev. 19,* 1–50.

Kato, V., and Kraml, M., 2005: *Geochemistry of Rwenzori hot springs*. Uganda, unpublished report, 13 pp.

Mahon, W., and Ellis, A.J., 1970: Chemistry in the exploration and exploitation of hydrothermal systems. *Geothermics, 2,* 1310-1322.

McNitt, J.R., 1982: The geothermal potential of East Africa. *Proceedings of the Regional Seminar on geothermal energy in Eastern and Southern Africa, Nairobi, Kenya,* 3-8.

Petrovic I., Heaney P.J., and Navrptsky A., 1996: Thermochemistry of the new silica polymorph moganite. *Phys. Chem. Minerals, 23***,** 119-126.

Reed, M.H., and Spycher, N.F., 1984: Calculation of pH and mineral equilibria in hydrothermal water with application to geothermometry and studies of boiling and dilution. *Geochim. Cosmochim. Acta, 48*, 1479-1490.

Tole, M.P., Ármannsson, H., Pang Zhonghe, Arnórsson, S., 1993: Fluid/mineral equilibrium calculations for geothermal fluids and chemical geothermometry. *Geothermics, 22,* 17-37.

Truesdell, A.H. 1976: Summary of Section III. Geochemical Techniques in Exploration. *Proceedings of the 2nd United Nations Symposium on the Development of Geothermal Resources, San Francisco*, 53-79.

Truesdell, A.H., 1991: Effects of physical processes on geothermal fluids. In: D'Amore, F. (coordinator), *Application of geochemistry in geothermal reservoir development.* UNITAR/UNDP publication, Rome, 71-92.

APPENDIX I: Analytical results if waters from the Buranga geothermal field

Sample ID	Location	pH	T	EC	TDS	F	Cl	Br	SO_4	HCO_3	CO_2	NH_3	SiO_2
UG-02-12	Kagoro	8.02	92.0	21600						2630,0			
UG-02-13	Nyansimbe	8.32	88,0	21600						2403,0			
UG-02-14	Mumbuga	8.12	96.0	19550						2183,0			
UG-93-09	Mumbuga	7.87	93.4		14600	27.9	3580	16.8	3720		2445		76.9
UG-93-10	Mumbuga	7.73	93.6		14030	27.2	3490	16.4	3570		2411		76.4
UG-93-11	Nyansimbe	7.61	80.3		17050	31.3	4160	20	4330		2889		88.6
UG-93-12	Kagoro	7.5	89		16400	30.8	4030	19.6	4160		2798		81
UG-93-13	Nyansimbe	7.81	85.8		17050	31.5	4240	20.4	4420		2878		85.7
UG-93-14	Nyansimbe	8.57	98.2		17080	31.3	4210	20.1	4400		2635		85.1
UG-93-16	Nyansimbe	8.15	95.8		16250	29.9	4010	19.3	4180		2638		87.7
UG-93-31	Kagoro	7.5	89.1								2739	3.5	
UG-93-32	Nyansimbe	8.58	97.3								2592	2.5	
UG-93-33	Mumbuga	7.9	93.6								2356	3	
UG-05-01	Mumbuga	8.7	94	17900			3133	14.9	3222	2850			70
UG-05-02	Nyansimbe	8.4	75.4	22400			4019	18.2	4186	3630			77.4
UG-05-03	Kagoro	8.6	88	21000			3735	16.9	3842	3360			76.6
UG-05-04	Buranga-BH	8.3	62	21500			3839	17.3	4001	3440			73.5

APPENDIX II: Analytical results of cations in waters from the Buranga geothermal field

Sample ID	Location	Li	Na	K	Mg	Ca	Sr	Mn	Fe	Al	B
UG-02-12	Kagoro						5.90				
UG-02-13	Nyansimbe						1.80				
UG-02-14	Mumbuga						6.00				
UG-93-09	Mumbuga	1.34	5320	195	2.13	2.45	2.41	0.001	0.04	0.021	4.3
UG-93-10	Mumbuga	1.3	5160	190	2.27	2.56	2.46	0.001	0.05	0.014	4.2
UG-93-11	Nyansimbe	1.51	6160	230	2.63	2.1	2	0.002	0.02	0.019	4.96
UG-93-12	Kagoro	1.47	5950	219	2.19	2.69	2.54	0.001	0.02	0.019	4.7
UG-93-13	Nyansimbe	1.54	6300	234	1.98	2.04	2.15	0	0.01	0.017	4.8
UG-93-14	Nyansimbe	1.51	6270	235	0.28	0.39	0.33	0.002	0.39	0.54	4.96
UG-93-16	Nyansimbe	1.48	5940	222	1.74	0.95	0.86	0.001	0.01	0.025	4.71
UG-05-01	Mumbuga	1.2	4716	166	.94	6.24	4.83	0.001	0.02	0,015	3.78
UG-05-02	Nyansimbe	1.51	5991	218	1.97	6.55	4.89	0.001	0.02	0,02	4.63
UG-05-03	Kagoro	1.41	5561	199	1.97	7.01	5.58	0.017	0.91	0.71	4.4
UG-05-04	Buranga-BH	1.45	5738	209	1.77	7.11	5.17	0.004	0.16	0.031	4.48

APPENDIX III: Analytical results for stable isotopes (‰) in waters from the Buranga and Katwe geothermal fields

Sample ID	Site name	Eastings	Northings	Altitude	Type	$\delta^{18}O$	$\delta^{2}H$
UG-02-12	Kagoro20	184031	91999	704	GTH	-3.70	-19.4
UG-02-13	Nyansimbe1	184248	92121	683	GTH	-3.53	-18.0
UG-02-14	Mumbuga5	184310	92183	684	GTH	-3.42	-16.5
UG-93-09	Mumbuga2				GTH	-3.6	-17.1
UG-93-10	Mumbuga5				GTH	-3.49	-12.8
UG-93-11	Nyansimbe13				GTH	-3.54	-12.4
UG-93-12	Kagoro20				GTH	-3.69	-12.7
UG-93-13	Nyansimbe19				GTH	-3.46	-12.9
UG-93-14	Nyansimbe17				GTH	-3.45	-13.4
UG-93-16	Nyansimbe9				GTH	-3.21	-12.2
UG-02-01	L.Kitagata2	830703	9992981	944	GTH	-0.74	2.4
UG-02-02	L.Kitagata5	830703	9992981	944	GTH	-0.80	-2.1
UG-02-11	Kibenge	172084	20719	1093	GTH	-4.46	-20.2
UG-93-06	L.Kitagata5				GTH	-0.73	0.5
UG-93-07	L.Kitagata2				GTH	-0.6	3.2
UG-93-18	L.Kitagata1				GTH	10	16.5
UG-93-27	L.Kitagata1				GTH	7.4	25.3
UG-94-06	L.Kitagata1	830703	9992981		GTH	2.2	0
UG-03-01	L.Kitagata2	830703	9992981		GTH	-0.86	-0.7
UG-03-02	L.Kitagata5	830703	9992981		GTH	-0.97	-0.7
UG-03-08	Kabuga1	171438	11293		GTH	-4.10	-15.2
UG-03-09	Kabuga2	171264	11364		GTH	-4.05	-13.9
UG-03-10	Kibenge1	172087	20727		GTH	-4.71	-18.4
UG-05-05	L.Kitagata2	830639	9993296		GTH		
UG-05-28	L.Katwe-5	9986777	820548	892	GTH	-4.84	-32.9
UG-05-65	Lusonga-BH	9986111	819742	896	GTH	-3.18	-12.7
UG-05-67	L.Kitagata-4	9993283	830640	923	GTH	-0.70	2.6
UG-05-68	L.Kitagata-6	9993283	830640	923	GTH	-0.74	1.6

APPENDIX IV: Analytical results for anions and stable isotopes in waters from the Kibiro geothermal field and northern Uganda

Sample ID	Site name	Type	pH	T (°C)	EC	TDS	F	Cl	Br	SO_4	CO_2	NH_3	SiO_2	H_2S	$\delta^{18}O$	$\delta^{2}H$
UG-99-01	Kibiro2	GTH	7.26	85	7210	4810	5.12	2500	16.7	46.7	146		129	10.7	-2.05	-11.1
UG-93-19	Mukabiga2	GTH	7.06	86.5		4576	5.12	2500	16.7	46.7	146		129	10.4	-2.01	-11.3
UG-93-20	Mukabiga5	GTH	7.14	81.1		4436	5.02	2450	16.4	26.4	155		125	13	-2.08	-11.8
UG-93-21	Mwibanda14	GTH	7.14	71.8		4384	4.74	2440	16.2	15.4	155		122	17.3	-1.98	-10.6
UG-93-22	Muntere15	GTH	8.05	39.5		4548	5.37	2580	17.3	49.9	115		135	0	-1.01	-3.9
UG-05-62	Amorpii	GHT	8.66	58	1790	890	5.2	470	1.5	26	71	2.1	73	5.61	-3.52	-7.7
UG-05-63	Okumu	GHT	8.45	45	1590	794	4.7	379	0.93	36	109	1.6	69	2.48	-3.29	-5.5
UG-05-64	Avuka-2	GHT	7.56	35	676	337	2.4	83	0.17	19	142	0.25	54	0	-2.5	1.9
UG-05-65	Lusoga BH	GHT	7.57	32	46300	23000	0.32	3385	22	3313	2218	10.7	53	0	-3.42	-7.3
UG-05-117	Amuru (Pakele)	GHT	9.06	49	449	nd	6.6	53	0.29	4.4	95.5	<0.1	70	0	-2.48	-1.9
UG-05-118	Amuru	GHT	8.23	48	508	nd	8	51	0.45	73	91.1	<0.1	68	0	-1.95	2.5
UG-05-58	Kanangorok-1	GHT	8.35	60	1631	815	12	95	<0.2	341	216	<0.1	118	0	-4.92	-18.8
UG-05-59	Kanangorok-2	GHT	8.39	42	1627	812	13.8	97	<0.2	343	207	<0.1	129	0	-4.83	-17.2
UG-05-60	Kanangorok-BH	BHW	8.44	38	1658	825	13	1658	<0.2	352	207	0.15	129	0	-4.88	-16.6

APPENDIX V: Analytical results for cations in waters from the Kibiro geothermal field and northern Uganda

Sample ID	Site name	Type	Li	Na	K	Mg	Ca	Cd	Sr	Mn	Fe	Al	B
UG-99-01	Kibiro2	GTH		1653	470	8.14	40			0.004	0	0.037	3.29
UG-93-19	Mukabiga2	GTH	1.5	1530	169	8.14	62		2.1	0.004	0	0.037	2.26
UG-93-20	Mukabiga5	GTH	1.48	1490	164	7.96	62.9		2.08	0.004	0.02	0.041	2.23
UG-93-21	Mwibanda14	GTH	1.46	1480	165	9.21	65.7		1.9	0.007	0	0.044	2.21
UG-93-22	Muntere15	GTH	1.53	1570	182	8.71	75.9		2.05	0.006	0.03	0.029	2.47
UG-05-62	Amoropii	GHT	0.12	352	10,9	0.36	4.5	0.0003	0.27	0.023	0.06		0.65
UG-05-63	Okumu	GHT	0.08	321	9.5	0.68	8.5	<0.0001	0.2	0.024	0.02		0.58
UG-05-64	Avuka-2	GHT	<0.05	138	7.3	3.1	8.4	<0.0005	0.07	0.011	0.02		0.22
UG-05-65	Lusoga BH	GHT	0.18	42	316	243	163	<0.001	2.4	0.87	1.2		0.85
UG-05-117	Amuru(Pakele)	GHT	<0.05	110	2.6	0.04	1.4	<0.00005	0.02	<0.005	0.1		<0.1
UG-05-118	Amuru	GHT	<0.05	111	3.9	0.76	6.6	<0.00005	0.07	<0	0.04		0.2
UG-05-58	Kanangorok-1	GHT	0.19	322	17.7	2.7	24	0.0022	0.77	<0055	0.08		0.18
UG-05-59	Kanangorok-2	GHT	0.2	323	19.2	1.5	21	0.0011	0.71	0.02	0.18		<0.1
UG-05-60	Kanangorok-BH	BHW	0.22	342	22	1.5	21	0.0009	0.73	0.12	0.32		0.76

APPENDIX VI: Analytical results for waters from Lake Kitagata, Kabuga and Kibenge hot springs

Sample ID	Site name	Type	pH	T	EC	TDS	Li	Na	K	Mg	Ca	Sr
UG-93-06	L.Kitagata5	GTH	8,41	66.6		27770	0.063	9310	644	0.85	0.6	0.6
UG-93-07	L.Kitagata2	GTH	8,03	56.6		19410	0.031	6510	523	6.27	1.45	1.3
UG-93-18	L.Kitagata1	GTH	9,57	61.2		244100	0.21	84200	4740	0.74	0.9	1.8
UG-93-27	L.Kitagata1	GTH	9.72	70.1		196000	0.07	66600	3500	1.38	4	1.7
UG-94-06	L.Kitagata1	GTH	9.33	61.1		99515	0.16	33600	1840	2	4.1	3.6
UG-03-01	L.Kitagata2	GTH	8.64	64,0	31800		0.0	8610	755	0.62	1.59	1.7
UG-03-02	L.Kitagata5	GTH	8.36	69.0	30900		0.05	8160	693	0.80	1.93	1.9
UG-03-08	Kabuga1	GTH	7.64	40.0	4050		0.079	624	29.4	21.1	197	1.8
UG-03-07	Rwagimba	GHT	6.87	69.2	6400	3190	0.59	1481	46	5.1	75	3.3
UG-03-09	Kabuga2	GTH	7.21	41.0	3560		0.063	537	21.6	12.8	198	1.5
UG-03-10	Kibenge1	GTH	7.25	47.0	3510		0.022	506	27.0	6.52	237	3.4
UG-05-05	L.Kitagata2	GTH	8.7	64	31300		0.048	9237	634	0.86	2.41	1.7

Sample ID	Site name	Mn	Fe	F	Cl	Br	SO_4	CO_2	NH_3	Al	SIO_2	B	H_2S
UG-93-06	L.Kitagata5	0.001	0.02	42	2430	14.2	13400	3105		0.01	91	0.82	0
UG-93-07	L.Kitagata2	0.001	0.01	26,7	1770	10.8	8970	2544		0.02	105	0.59	0
UG-93-18	L.Kitagata1	0.012	0.02	402	20900	120	108900	17785		0.07	351	7.6	40.7
UG-93-27	L.Kitagata1	0.005	0.03	310	16900	89.8	85300	5248	5.7	0.8	289.8	5.2	7.1
UG-94-06	L.Kitagata1	0.003	0.025	162	8370	44.8	44000	10350	3.5	0.48	210	2.77	19.4
UG-03-01	L.Kitagata2	0.014	0.00	65,6	2400	14	13000	8206		0.1	66.1	0.78	
UG-03-02	L.Kitagata5	0.016	0.00	63,1	2300	13	13000	7268		0.1	66.1	0.71	
UG-03-08	Kabuga1	0.151	0.00	5,3	590	5.3	1100	377		0	38.3	0.33	
UG-03-07	Rwagimba	0.11	0.8	8	905	4.1	1527	651	<0.1		65	0.94	0
UG-03-09	Kabuga2	0.186	0.00	6,1	200	4.5	430	338		0.01	47.1	0.28	
UG-03-10	Kibenge1	0.161	0.00	7,6	560	4.5	870	247		0.01	43	0.38	
UG-05-05	L.Kitagata2	0.017	0.02		2447	13.4	12959	4160		0.02	81.7	0.82	

APPENDIX VII: Ratios of different conservative elements in waters in Katwe, Kabuga, Kibenga and Rwagimba waters

Sample ID	Site name	Na/Cl	CL/Br	Cl/Li	CL/B	Na/B	K/Na	Na/K	Cl/18O
UG-93-06	L.Kitagata5	3.8	171.1	38571.4	2963.4	11353.7	0.07	14.5	-3328.8
UG-93-07	L.Kitagata2	3.7	163.9	57096.8	3000.0	11033.9	0.08	12.4	-2950.0
UG-93-18	L.Kitagata1	4.0	174,2	99523.8	2750.0	11078.9	0.06	17.8	2090.0
UG-93-27	L.Kitagata1	3.9	188.2	241428.6	3250.0	12807.7	0.05	19.0	2283.8
UG-94-06	L.Kitagata1	4.0	186.8	52312.5	3021.7	12130.0	0.05	18.3	3804.5
UG-03-01	L.Kitagata2	3.6	171.4	54545.5	3076.9	11038.5	0.09	11.4	-2790.7
UG-03-02	L.Kitagata5	3.5	176.9	46000.0	3239.4	11493.0	0.08	11.8	-2371.1
UG-03-08	Kabuga1	1.1	111.3	7468.4	1787.9	1890.9	0.05	21.2	-143.9
UG-05-07	Kabuga 1	1.3	107.1	7419.35	1277.78	1627.78	0.03	31.7	
UG-03-09	Kabuga2	2.7	44.4	3174.6	714.3	1917.9	0.04	24.9	-49.4
UG-03-10	Kibenge1	0.9	124.4	25454.5	1473.7	1331.6	0.05	18.7	-118.9
UG-05-08	Kibenge1	0.94	139.29	2647.06	1218.75	1145.83	0.04	22.63	
UG-05-05	L.Kitagata2	3.8	182,6	50979.2	2984.1	11264.6	0.07	14.6	-118.9
	Rwagimba 1	1.77	171.02	1853.98	1180.28	2084.51	0.03	35.53	

APPENDIX VIII: Ratios of different conservative elements in waters from the Buranga geothermal hot springs

Sample ID	Location	Cl/Br	Cl/^{18}O	Na/Cl	Cl/B	Cl/Li	K/Na	Na/K	Na/B
UG-93-09	Mumbuga	213.10	-994.44	1.49	832.56	2671.64	0.04	27.28	316.67
UG-93-10	Mumbuga	212.80	-1000.00	1.48	830.95	2684.62	0.04	27.16	314.63
UG-93-11	Nyansimbe	208.00	-1175.14	1.48	838.71	2754.97	0.04	26.78	308.00
UG-93-12	Kagoro	205.61	-1092.14	1.48	857.45	2741.50	0.04	27.17	303.57
UG-93-13	Nyansimbe	207.84	-1225.43	1.49	883.33	2753.25	0.04	26.92	308.82
UG-93-14	Nyansimbe	209.45	-1220.29	1.49	848.79	2788.08	0.04	26.68	311.94
UG-93-16	Nyansimbe	207.77	-1249.22	1.48	851.38	2709.46	0.04	26.76	307.77
UG-05-01	Mumbuga	210.27		1.51	828.84	2610.83	0.04	28.41	316.51
UG-05-02	Nyansimbe	220.82		1.49	868.03	2661.59	0.04	27.48	329.18
UG-05-03	Kagoro	221.01		1.49	848.86	2648.94	0.04	27.94	329.05
UG-05-04	Buranga-BH	221.91		1.49	856.92	2647.59	0.04	27.45	331.68

APPENDIX IX: Ratios of conservative elements in waters from Kibiro and Northern Uganda hot springs

Sample ID	Location	Na/Cl	CL/BR	CL/B	Na/K	Li/B
UG-99-01	Kibiro	0.66	149.7	759.88	3.517	
UG-01-10	Kibiro	0.53			8.167	0.00
UG-01-11	Kibiro	0.54			7.760	
UG-93-19	Mukabiga	0.61	149.7	1106.19	9.053	
UG-93-20	Mukabiga	0.61	149.4	1098.65	9.085	0.65
UG-93-21	Mwibanda	0.61	150.6	1104.07	8.970	0.65
UG-93-22	Muntere	0.61	149.1	1044.53	8.626	0.69
UG-05-62	Amoropii	0.75	313.3	723.08	32.294	0.05
UG-05-63	Okumu	0.85	407.5	653.45	33.789	0.12
UG-05-64	Avuka-2	1.66	488.2	377.27	18.904	
UG-05-65	Lusoga BH		0.0	0.00	0.133	0.82
UG-05-117	Amuru (Pakele)	2.08	182.8			
UG-05-118	Amuru	2.18	113.3	255.00	28.462	
	Kanangorok-1	3.39		527.78	18.192	0.95
	Kanangorok-2	3.33			16.823	1.11
	Kanangorok-BH			0.00	15.545	